This is to certify that the

thesis entitled

Evaluation of Analytical Formulas for Calculating Cyclotron Orbit Properties

presented by

Dong-O Jeon

has been accepted towards fulfillment
of the requirements for

M. S. degree in Physics

M. M. Gordon

Major professor

Date May 17, 1990

EVALUATION OF ANALYTICAL FORMULAS FOR CALCULATING CYCLOTRON ORBIT PROPERTIES

By

Dong-o Jeon

A DISSERTATION

Submitted to
Michigan State University
in partial fulfillment of the requirements
for the degree of

MASTER OF SCIENCE

Department of Physics and Astronomy

1990

ABSTRACT

EVALUATION OF ANALYTICAL FORMULAS FOR CALCULATING CYCLOTRON ORBIT PROPERTIES

By

Dong-o Jeon

Improved analytical formulas for calculating cyclotron orbit properties have recently been derived by M. M. Gordon. To test these formulas, a computer program has been written that uses magnetic field data from any cyclotron to evaluate these formulas and to compare the results with those obtained from a standard orbit integration code. This investigation has employed field data from three different superconducting cyclotrons all having magnet poles with three sectors. The results show that the formulas give the best results in those cases where the average magnetic field is relatively high (45 kilogauss). They also show that the new formulas are much more accurate than the old simpler formulas.

To Father, my parents, brothers and Chris Park

ACKNOWLEDGMENTS

I'd like to express my deep appreciation for the invaluable and painstaking advice and kindness of Dr. Gordon. I'd like to thank Dr. Blosser and Dr. Mahanti and F. Marti for their concern and time. I also like to thank S. G. Kim for his kind advice on how to use a word processor.

Contents

List of Figures

Chapter 1

Introduction

In determining whether a given magnetic field meets the performance requirements for accelerating a particular ion to a given final energy, one must calculate various orbit properties of the given field as a function of energy or radius. The most important of these properties are the orbit period τ, and the radial and vertical tunes, ν_r and ν_z.

Such calculations can be carried out either numerically, using the Equilibrium Orbit Code [1] or by analytical formulas. The accuracy of the the E. O. Code is excellent, but it does not provide the insight into the effects of various field characteristics which is provided by the analytical formulas.

Cyclotron orbit properties have been analyzed by many authors [2, 3, 4] in the past and although the resulting formulas have proved useful,their accuracy is quite limited particularly when applied to machines with only three sectors. Dr. M. M. Gordon has undertaken the task of deriving more accurate formulas by introducing certain improvements. First of all, his analysis systematically maintains all terms, whether large or small, that are of second order in the flutter field, that is, the part of the field that varies with the azimuth θ. In doing so, an improved first-order calculation of the equilibrium orbits themselves is made use of. Finally, the values of ν_z and ν_r are calculated using a formula which is derived from a second-order Born approximation

and which should be valid all the way to the stop-band limit, $\nu = N/2$, where N is the number of sectors.

The purpose of this thesis is to test these new analytical formulas by applying them to field data from various cyclotrons and comparing the results with those obtained from the Equilibrium Orbit Code.

All the theoretical formulas used in this paper are briefly summarized in Ch. 2 while a detailed discussion of their derivation is presented in the Appendix.

The theory uses a reference radius as an independent variable which is the radius where various Fourier coefficients and their derivatives are calculated. In contrast, the customary E. O. Code uses energy as an independent variable. Thus it is necessary to match these two independent variables to make a proper comparison between the results. The solution of this problem is described in Ch. 3 on the computer program.

We use field data from three cyclotrons to test how well the results obtained from the analytical formulas agree with those obtained from the E. O. Code. The results of these comparisons are discussed in Ch. 4. As will be seen, the theory works very well for superconducting cyclotrons operating close to bending limit of their magnets. In such cases, the magnitude of the flutter field is small compared with that of the average magnetic field.

As a by-product of this thesis, a small improvement in the E. O. Code has been derived which removes certain fluctuations that occur in plots of ν_z and ν_r as a function of radius (or energy). Specifically, this improvement provides a more accurate method of calculating the radial derivatives of the field data.

Chapter 2

Theoretical Formulas

The analytical formulas were calculated by M.M.Gordon and are presented in more detail in the Appendix.

We assume that the median-plane magnetic field is represented by:

$$\begin{aligned} B(r,\theta) &= B_0(r) + \sum_n [\, G_n(r)\sin n\theta + H_n(r)\cos n\theta \,] \\ &= B_0(r) + \sum_n B_n(r)\cos[\, n(\,\theta - \beta_n(r)\,)\,] \end{aligned} \tag{2.1}$$

where n = N, 2N,..., and N is the number of sectors in the cyclotron magnet.

All the theoretical formulas are expressed in terms of certain field parameters at a given value of r, namely :

$$f_n = \frac{B_n}{B_0} \tag{2.2}$$

$$t_n = r\left(\frac{d\beta_n}{dr}\right) \tag{2.3}$$

$$k_n = \frac{r}{B_0}\left(\frac{dB_n}{dr}\right) \;, k_0 = \frac{r}{B_0}\left(\frac{dB_0}{dr}\right) \;, \tag{2.4}$$

$$k'_n = \frac{r^2}{B_0}\left(\frac{d^2B_n}{dr^2}\right) \;, k'_0 = \frac{r^2}{B_0}\left(\frac{d^2B_0}{dr^2}\right) \;, \tag{2.5}$$

$$k''_0 = \frac{r^3}{B_0}\left(\frac{d^3B_0}{dr^3}\right) \;. \tag{2.6}$$

I Momentum and Energy

We take the charge and mass of the particle to be q and m, and define the dimensionless parameter λ as follows:

$$\lambda = \frac{qrB_0(r)}{mcp} \ , \tag{2.7}$$

where p is the momentum expressed in mc units so that $p = \gamma\beta$.

The value of λ is found by iteration from the formula (see eq. A.22 in the Appendix):

$$1 - \lambda = \frac{1}{4}\lambda^2 \sum_n \left[(3f_n + 2k_n)\, y_n + \frac{1}{2} M''\, y_n^2 \right] \tag{2.8}$$

where

$$y_n = \frac{f_n}{n^2 - \mu^2} \tag{2.9}$$

are Fourier coefficients measuring the deviation of the orbit from a circle (see eq. A.10 and eq. A.21 in the Appendix), and

$$M'' = \lambda (2k_0' + 7k_0 + 3) \ .$$

Also, as described in sec. VII of the Appendix, the value of μ is obtained from:

$$\sin^2(\mu\theta_0/2) = \sin^2(\kappa\theta_0/2) + \frac{1}{2}(\theta_0/2)^2 \frac{\sin\kappa\theta_0}{\kappa\theta_0} \sum_n \left[\frac{g_n^2}{n^2 - 4\kappa^2} \right] \tag{2.10}$$

where $\theta_0 = 2\pi/N$,

$$\kappa^2 = M'$$

with

$$M' = \lambda(1 + k_0) + \frac{1}{2}(\lambda - 1)$$

and

$$g_n^2 = \frac{1}{4}\lambda^2 \left[(3f_n + 2k_n)^2 + 4(nf_n t_n)^2 \right]. \tag{2.11}$$

The final value of λ determines the momentum p and hence the energy E:

$$E = \frac{p^2}{1+\sqrt{1+p^2}} \times mc^2 \ . \tag{2.12}$$

II Frequency Error

The Equilibrium Orbit is discussed in sec. II in the Appendix. Define τ to be the orbit period and $\omega = 2\pi/\tau$.

As shown in eq. A.26 of the Appendix, the frequency error is given by

$$\frac{\omega_0}{\omega} - 1 = \frac{r\omega_0}{\beta c}\left[1 + \frac{\lambda^2}{8}\sum_n \left(2n^2+1\right) y_n^2\right] - 1 \tag{2.13}$$

where $\beta = \frac{p}{\sqrt{1+p^2}}$ and ω_0 is a fixed reference frequency, and y_n is given in eq. 2.9 above.

III Radial and Vertical Oscillations

As shown in sec. VI of the appendix, the formula for the tune ν is given as follows:

$$\sin^2\left(\nu\theta_0/2\right) = \sin^2\left(\kappa\theta_0/2\right) + \frac{1}{2}\left(\frac{\theta_0}{2}\right)^2\left(\frac{\sin\kappa\theta_0}{\kappa\theta_0}\right)\sum_n\left[\frac{g_n^2}{n^2-4\kappa^2}\right] \tag{2.14}$$

where $\theta_0 = 2\pi/N$ is the period and both g_n and κ are given below for radial and vertical oscillations. Note that this formula is the same as that used for calculating μ in eq. 2.10 above.

Caution is necessary when $\kappa \rightarrow N/2$,because the sum has a singular term in this case. The singularity is removed by the $\sin\kappa\theta_0$ in front of the sum. Thus, if $\kappa = N(1-\epsilon)/2$,then

$$\frac{\sin\kappa\theta_0}{N^2-4\kappa^2} = \frac{\sin\pi\epsilon}{N^2(2-\epsilon)\epsilon}$$

which approaches $\pi/2N^2$ when $\epsilon \rightarrow 0$. One should therefore test whether $\epsilon < 10^{-3}$, say, and revise the sum accordingly.

Note further that if $\kappa^2 < 0$, then

$$\sin^2(\kappa\theta_0/2) \;\rightarrow\; -\sinh^2(|\kappa|\,\theta_0/2)$$

and

$$\frac{\sin\kappa\theta_0}{\kappa\theta_0} \;\rightarrow\; \frac{\sinh\,|\kappa|\,\theta_0}{|\kappa|\,\theta_0}$$

in the above formula for ν.

A Radial Oscillations

As shown in sec. IV of the Appendix, the values of κ_x^2 and g_n^2 in this case are

$$\kappa_x^2 \;=\; \lambda(1+k_0) + \frac{1}{2}\lambda^2\sum_n y_n\left(f_n + 3k_n + k_n' - n^2 f_n t_n^2\right) +$$

$$\frac{1}{8}\lambda^2\left[6\lambda(1+k_0) - 1\right]\sum_n n^2 y_n^2 + \frac{1}{8}\lambda^3(1 + 11k_0 + 11k_0' + 2k_0'')\sum_n y_n^2, \tag{2.15}$$

$$(g_x)_n^2 \;=\; \lambda^2\left\{(nf_nt_n)^2 + \left[f_n + k_n + y_n\left(\frac{1}{2}n^2 + \lambda(1 + 3k_0 + k_0')\right)\right]^2\right\}, \tag{2.16}$$

where $(g_x)_n^2$ is obtained from squaring the eq. A.36 of the Appendix and taking the average over θ and then multiplying by a factor of two.

B Vertical Oscillations

As shown in sec. V of the appendix, the values of κ_z^2 and g_n^2 are given by

$$\kappa_z^2 \;=\; -\lambda k_0 + \frac{1}{2}\lambda^2\sum_n\left(n^2 f_n + n^2 f_n t_n^2 - 2k_n - k_n'\right)y_n -$$

$$\frac{1}{8}\lambda^2\left[1 + 2\lambda k_0\right]\sum_n n^2 y_n^2 - \frac{1}{8}\lambda^3(6k_0 + 9k_0' + 2k_0'')\sum_n y_n^2, \tag{2.17}$$

$$(g_z)_n^2 \;=\; \lambda^2\left\{(nf_nt_n)^2 + \left[k_n + \left(\frac{1}{2}n^2 + 2\lambda k_0 + \lambda k_0'\right)y_n\right]^2\right\} \tag{2.18}$$

where $(g_z)_n^2$ is obtained from squaring the eq. A.39 of the Appendix and taking the average over θ and then multiplying by a factor of two.

Chapter 3

Computer Program Description

The analytical formulas make use of the Fourier coefficients and their derivatives. Because the field data are given on a polar grid having a uniform Δr and a uniform $\Delta\theta$, the Fourier coefficients in eq. 2.1 above are computed as a function of radius from the data given on each radial grid point, and their derivatives as a function of radius are determined from these coefficients.

I Determining Fourier Coefficients

The Fourier coefficients of various harmonic numbers are obtained from numerical integration. More precisely, the trapezoidal method is used.

Since the field data are given at $\theta = 0^o, 1^o, 2^o, \ldots$, the Fourier coefficients in eq. 2.1 are obtained from the following formula:

$$H_n(r) = 2\sum_{i=1}^{N_{th}} \left[B(r, \frac{(i-1)\pi}{180}) \cos(n\frac{(i-1)\pi}{180}) \right] / N_{th} \tag{3.1}$$

$$G_n(r) = 2\sum_{i=1}^{N_{th}} \left[B(r, \frac{(i-1)\pi}{180}) \sin(n\frac{(i-1)\pi}{180}) \right] / N_{th} \tag{3.2}$$

where $N_{th} = 360/N$ is the number of θ values within one sector, with N being the

number of sectors.

The amplitude of the n^{th} harmonic,$B_n(r)$, is obtained from:

$$B_n(r) = \sqrt{G_n^2(r) + H_n^2(r)} \ . \tag{3.3}$$

We have harmonic numbers n that are multiples of N since the field has N- fold azimuthal symmetry. Of course this is an idealization, since real field data include imperfections.

II Derivatives of Coefficients

The data are given for $0 \leq r \leq r_{max}$ at values that are multiples of Δr. We calculate the first derivative using a three-point formula. That is, for an arbitrary function $F(r)$, we use:

$$\frac{dF(r)}{dr} = \frac{F(r+\Delta r) - F(r-\Delta r)}{2\Delta r} \ . \tag{3.4}$$

This formula is used to calculate the first derivative of B_0, B_n, G_n, H_n and used in calculating k_0 and k_n defined in eq. 2.4 and in calculating t_n from the following:

$$nf_n t_n = \frac{1}{B_n}\left[H_n G_n' - G_n H_n' \right] \tag{3.5}$$

where $G_n' = \frac{r}{B_0}\left(\frac{dG_n}{dr}\right)$ and $H_n' = \frac{r}{B_0}\left(\frac{dH_n}{dr}\right)$.

After the first derivatives have been calculated at each r value, the second derivatives are obtained from the same formula by replacing F by $\frac{dF}{dr}$. The second derivatives are then used to evaluate k_0' and k_n' in eq. 2.5. Third derivatives of B_0 required for calculating k_0'' in eq. 2.6 are obtained in the same manner.

We lose one point at $r = r_{max}$ in calculating first derivatives, a second one at $r = r_{max} - \Delta r$ in calculating second derivatives, and so on. The extra points needed beyond $r = 0$, that is,at $r = -\Delta r$, $-2\Delta r$, and $-3\Delta r$, can be obtained by symmetry.

III Interpolation Used in E. O. Code

Because the E. O. Code uses numerical integration, it requires values of B, $\frac{\partial B}{\partial r}$, and $\frac{\partial B}{\partial \theta}$ at values of r that are not on the grid points where the field data are given. Interpolation is therefore required and the method adopted for this code is somewhat different from the usual four-point Lagrange form.

When a function $F(r)$ is given at four evenly spaced points (r_1, r_2, r_3, r_4), the values of the function between r_2 and r_3 is found as follows. First of all, using the left three points (r_1, r_2, r_3), we calculate $F_1(r)$ using a three-point Lagrange formula, and then use the right three points (r_2, r_3, r_4) to calculate $F_2(r)$ again using the three-point fromula. The function is then obtained by a linearly weighted average of these two values:

$$F(r) = \frac{r - r_2}{\Delta r} F_2(r) + \frac{r_3 - r}{\Delta r} F_1(r) \tag{3.6}$$

where $\Delta r = r_3 - r_2$. The resultant function $F(r)$ is not only continuous at $r = r_2$ and r_3, but also has a continuous first derivative at these points. However, the second derivative is not continuous. The original E. O. Code uses this formula to find not only the field, but also its first derivative at each r value. As a result, the values of ν_z, which are sensitive to the first derivatives, exhibit small cusps when plotted as a function of energy or radius.

To remedy this problem, the method used to find first derivatives was changed to the following. First, a table of first derivatives was constructed at the grid points using the eq. 3.4 for $\frac{dF}{dr}$. We then use eq. 3.6 to interpolate in this table to find the derivative at the given r values. This not only cures the difficulty, but is also consistent with the method already used in the E. O. Code for finding first derivatives of the field with respect to θ at a given r value.

The Lagrange interpolation formulas can be found in ref. [5].

IV Matching the Theory and E. O. Code

Energy is used as an independent variable in the case of the Equilibrium Orbit Code while the radius called reference radius is used as an independent variable for the theory. In order to avoid interpolating in the theoretical values, we therefore modified the E. O. Code to provide output at the same values of the reference radius defined in eq. A.11 of the Appendix.

This is accomplished as follows:

1. Using a fixed energy step, the E. O. Code is run to obtain a table giving the reference radius and other orbit properties as a function of radius. The fixed energy step is chosen small enough to insure the accuracy of the interpolation required at step 3 below.

2. Using the analytical formulas given in Ch. 2, the program then calculates all of the orbit properties, including the energy, for each value of the radius.

3. The program then interpolates in the table of E. O. data to find the energy corresponding to the given reference radius, and then reruns the E. O. Code at this energy to obtain the corresponding orbit properties including the reference radius. The program then checks whether the difference in radius values falls within an acceptible error, 1×10^{-5} inch.

4. For each value of the radius, the program then compares the values of E, τ, ν_r and ν_z obtained from the analytical formulas with those from the E. O. Code.

Chapter 4

Data Analysis

Here we deal with three sets of field data with various characteristics. First there is the field of the Harper Hospital cyclotron, second the 130 MeV/A, $q/A = 0.33$ field of the K1200 cyclotron and third the 200 MeV proton field of the cyclotron being designed at Orsay, France. All these are superconducting cyclotrons with magnet poles having three sectors.

The difference for an arbitrary quantity, F, is defined as follows:

$$\Delta F = F_{E.\ O.\ Code} - F_{Theory} \tag{4.1}$$

where F will be E, τ, ν_r, ν_z. Also $(\Delta E)/E$ and $\Delta\tau/\tau$ are defined as follows:

$$(\Delta E)/E = \left(E_{E.\ O.\ Code} - E_{Theory} \right) / E_{E.\ O.\ Code} , \tag{4.2}$$

$$(\Delta\tau)/\tau = \left(\frac{\omega_0}{\omega_{E.\ O.\ Code}} - \frac{\omega_0}{\omega_{Theory}} \right) / \frac{\omega_0}{\omega_{E.\ O.\ Code}} . \tag{4.3}$$

Because the field data are given on polar mesh, there are only a limited number of harmonics which have significance, that is, we have at most 120 independent Fourier coefficients because at each value of radius only 120 azimuthal points were measured. The maximum number of harmonics added in the theory is chosen such that there would be no change in the output when an extra harmonic is added.

I The Field of the Harper Cyclotron

The Harper cyclotron which is a superconducting cyclotron constructed at MSU has the following characteristics.

It is designed to accelerate deutrons to a final energy of around 50 MeV. The field data are given on a polar mesh with $\Delta r = 0.1$ inch and $\Delta\theta = 1^o$, and the maximum radius given is 12.3 inches. The magnitude of the central magnetic field is 45.9 kGauss.

The number of harmonics computed is ten, so that $n_{max} = 30$.

Figure 4.1 shows the magnitude of the three leading f_n for $n = 3, 6, 9$ (refer to eq. 2.2). As you can see, the fractional magnitude of f_3 is the largest with maximum value of around 0.18. The magnitudes of the 6^{th} and 9^{th} harmonics are smaller with maximum values of 0.05 and 0.02 respectively. These characteristics are favorable relative to a theory which assumes the orbits to be nearly circular. Figure 4.1 also shows plots of t_n for $n = 3, 6, 9$ (refer to eq. 2.3). As can be seen, these are quite linear up to the radius of 11 in. for the third and sixth harmonics. At $r = 6$ in. , t_9 shows the effect of a 180^o phase shift associated with a zero crossing of f_9. (The theoretical formulas are functions of f_n^2 rather than f_n).

Figure 4.2 shows the plots of k_n for $n = 0, 3, 6, 9$ (refer to eq. 2.4). The plot of k_0 starts out from zero and increases up to a maximum value of 0.12 near $r = 12$ inches. The curve of k_3 starts out from 0.10 and at larger radii falls to a minimum of -0.70, and this curve decreases sharply from the radius of around 10 inches. The maximum value of k_6 is 0.04 and the minimum is -0.12. The maximum of k_9 is 0.08 and the minimum is -0.02.

Figure 4.3 shows the plot of $(\Delta E)/E$ and $(-\Delta\tau/\tau)$ both in the units of 10^{-5}. Note a change of scale by the factor of 10 at the radius of 10 inches. Clearly these

fractional differences are very small up to the radius of 10 inches (corresponding to the energy of 33 MeV). In the last quarter inch (46 MeV to 48 MeV), these quantities change quite rapidly. Note the similar patterns of behaviour of the two curves with the magnitude of the fractional difference of energy being approximately twice as large as that of the fractional period difference. The polarity of the small fluctuations of these two curves is also the same, that is, when one curve has a small upward peak, the other has a small upward peak,too.

Note that since $\tau \approx 2\pi r/v$, the following equation holds:

$$-\frac{\Delta\tau}{\tau} \approx \frac{\Delta v}{v} \approx \frac{1}{2}\frac{\Delta E}{E} \ . \tag{4.4}$$

This is why we have the factor of around 2 between $(\Delta E)/E$ and $-(\Delta\tau)/\tau$.

Figure 4.4 shows the curve of $\Delta\nu_r$ in the units of 10^{-4} on top and that of $\Delta\nu_z$ in the units of 10^{-3} at the bottom. Both $\Delta\nu_r$ and $\Delta\nu_z$ show the same patterns of behaviour with the magnitude of $\Delta\nu_z$ being about five to ten times as large as that of $\Delta\nu_r$. This is not surprising since the theory involves ν_z^2, and one should compare $\nu_z(\Delta\nu_z)$ with $\Delta\nu_r$. That is, the values of ν_r always lie between 0.99 and 1.04, while the values of ν_z start out close to zero and then rise to a plauteau with $\nu_z = 0.2$ between 9 to 11 in. ,and finally rise to 0.32 at 12 inches.

Note that the polarity of the fluctuations on the $\Delta\nu_z$ curve and on the $\Delta\nu_r$ curve is opposite, that is, if one curve has a little sharp upward peak then the other one has a little sharp downward peak. This is due to the fact that most of the terms in the formula for κ_z^2 appear with opposite sign in the formula for κ_x^2 (refer to eq. 2.17 and eq. 2.15). All four of the figures show erratic behaviour around the radius of 6 in., and between 10 to 12 inches. This can be attributed to the defects in the magnetic field data which were derived from field measurements. Another trend worthy of note is that the plots of $\Delta\nu_z$ and $\Delta\nu_r$ are positive over most range of the radii.

Figure 4.5 shows the plot of ν_r above that of ν_z. As can be seen, the radius of 12 in. corresponds to the extraction region. The small bump around the radius of 6 in. is observed in both of the plots and is due to the defects in the field data.

Figure 4.6 shows the plot of $\Delta\nu_z$ between the ν_z from the E. O. Code and that from the theory by M. M. Gordon, and the plot of $\Delta\nu_z$ between the ν_z from the E. O. Code and that from the theory by Hagedoorn and Verster [4]. Both of them are in the units of 10^{-3}. As can be observed, the error of the analytical results by Hagedoorn and Verster becomes larger as the energy of a particle increases, which means that the particle becomes more and more relativistic, because the theory [4] assumes that the particle is slow enough for the relativistic effects to be neglected, and the formulas for the vertical tune do not have any term like k_0''.

According to the theory by Hagedoorn and Verster [4], the expression for ν_z^2 is given as follows:

$$\nu_z^2 = -\bar{\mu}' + \sum_n \left[\frac{n^2(A_n^2 + B_n^2)}{2(n^2-1)} - \frac{A_n A_n' + B_n B_n'}{2(n^2-1)} - \frac{A_n A_n'' + B_n B_n''}{2(n^2-1)} + \frac{(A_n')^2 + (B_n')^2}{2n^2} \right] \tag{4.5}$$

where

$$\bar{\mu}'(r) = \frac{r}{B_0(r)} \frac{dB_0(r)}{dr} , \tag{4.6}$$

$$A_n'(r) = r\left(\frac{dA_n(r)}{dr}\right) , B_n' = r\left(\frac{dB_n(r)}{dr}\right) , \tag{4.7}$$

$$A_n''(r) = r^2\left(\frac{d^2A_n(r)}{dr^2}\right) , B_n''(r) = r^2\left(\frac{d^2B_n(r)}{dr^2}\right) , \tag{4.8}$$

and the median plane magnetic field is given by:

$$B(r,\theta) = B_0(r)\left[1 + \sum_n \left(A_n(r)\cos n\theta + B_n(r)\sin n\theta \right)\right] . \tag{4.9}$$

The expression for ν_z^2 is different from that given in the paper by Hagedoorn and Verster in that the sign of the third term in the summation changed from plus to minus when it was rederived. For more datails, refer to the paper by Hagedoorn and Verster [4].

II 130 MeV/A Field of the K1200 Cyclotron

Presented here are the 130 MeV field data of the superconducting K1200 cyclotron [6] at MSU designed to accelerate an ion with $q/A = 0.333$, where A is the number of nucleons, to the final energy of 130 MeV per nucleon. $\Delta r = 0.5$ in. and $\Delta\theta = 1^o$ and the maximum value of radius given is 44 inches. The extraction radius is around 40 inches. The magnitude of the central magnetic field is around 44.5 kGauss.

The number of harmonics calculated is ten, so that $n_{max} = 30$ again.

Figure 4.7 shows the plots of f_n (refer to eq. 2.2) and t_n (refer to eq. 2.3) for $n = 3, 6, 9$. The maximum magnitude of f_3 is around 0.2 and those of f_6 and f_9 are 0.05 and 0.02 respectively. Their values form a plateau from 10 to 32 inches. The plots of t_n for $n = 3, 6, 9$ show similar patterns of behaviour. They decrease linearly up to the radius of around 38 in. and then start to increase. Note that the magnitudes of f_n of this 130 MeV field data are almost equal to those of the Harper cyclotron field data (refer to figure 4.1).

Figure 4.8 shows the plots of k_0 and k_n for $n = 3, 6, 9$ (refer to eq. 2.4). The plot of k_0 starts out from zero and increases with a periodic ripple on it and reaches its maximum of 0.30 at 38 in. and then decreases sharply afterwards. The plot of k_3 forms a plateau with a periodic ripple on it and then decreases sharply from around 36 in. down to -0.5. The plot of k_6 is almost constant with a fluctuation on it and decreases sharply from around 34 in. down to -0.18. The plot of k_9 is almost constant up to the radius of 36 in. and has a bump with maximum value of 0.20.

Figure 4.9 shows the plot of $(\Delta E)/E$ on top of that of $-(\Delta\tau)/\tau$ with both in the units of 10^{-5}. The reason the values of $(\Delta E)/E$ are very large when the radius is small is that when the radius is small, E is almost equal to zero and hence the error is amplified. Again they show similar patterns of behaviour besides that the

magnitude of $(\Delta E)/E$ is about 2 to 3 times as large as that of $-(\Delta\tau)/\tau$, which is quite natural (see eq. 4.4). The polarity of the fluctuation of these two curves is the same, which is true for the Harper cyclotron field. Note the periodic ripples with a period of about 3 in. which is well correlated with the gaps between the trim coils. The general trend of these two curves is decreasing up to the radius of around 35 in. (95 MeV), and then the curves start to increase rapidly and become positive eventually. It should be noted that the values of these two quantities, averaging out the fluctuation, are negative while those of the medical cyclotron field are positive. Because the magnitudes of f_n and k_n of these two sets of field data are almost the same, $(\Delta E)/E$ and $-(\Delta\tau)/\tau$ of these sets of data are almost of the same magnitude.

Figure 4.10 shows the plot of $\Delta\nu_r$ in the units of 10^{-4} on top of that of $\Delta\nu_z$ in the units of 10^{-3}. As is true in the case of fractional energy difference and fractional period difference, rather remarkable behaviour of periodicity is observed which is well correlated with the gaps between the trim coils. The values of these are positive, averaging out the fluctuations over most of the range of radius. The polarity of the fluctuation of these two curves is opposite, which is quite natural because most of the terms appearing in κ_z^2 (refer to eq. 2.17) are appearing with opposite sign in κ_x^2 (refer to eq. 2.15). Because the field parameters such as f_n and k_n are almost of the same magnitude as those of the Harper cyclotron field data, the values of $\Delta\nu_z$ and $\Delta\nu_r$ of these two sets of field data are of the same magnitude.

Figure 4.11 shows the plots of ν_z and ν_r. Observe that the amplitude of the ripple on the ν_z curve is larger than that on the ν_r curve. This is probably due to the fact that ν_z is sensitive to the first derivative of the field. This periodic ripple is well correlated with the gaps between the trim coils.

Figure 4.12 shows the plot of ν_z of the E. O. Code and that of the theory by M. M. Gordon above the plot of ν_z of the E. O. Code and that of the theory by

Hagedoorn and Verster. As shown, there is some range of radius where the theory by Hagedoorn and Verster predicts imaginary values of ν_z which are plotted as negative values while both of the E. O. Code and the theory by M. M. Gordon produce real ν_z values. Clearly the new theory of M. M. Gordon is an improvement of the theory by Hagedoorn and Verster. For the expression of ν_z^2, refer to eq. 4.5.

III The Field Data of the Orsay Cyclotron

These field data originate from the cyclotron being designed in Orsay, France [7] to accelerate protons to a final energy of 200 MeV with the magnitude of the central magnetic field 20.2 kGauss which is about twice as small as those of the two previously discussed fields. The Δr is 2 cm, $\Delta\theta$ is 2^o, and the maximum radius of field data is 1.48 meter. The extraction radius corresponds to the radius of around 90 cm.

The number of harmonics computed is fifteen, so that $n_{max} = 45$.

Figure 4.13 shows the plots of f_n and t_n for $n = 3, 6, 9$. What is unusal is that the magnitude of f_9 is larger than that of f_6. The magnitudes of f_n for $n = 3, 6, 9$ start to decrease sharply from around 70 cm and are about two times as large as those of the two previous sets of field data. The values of t_n for $n = 3, 6, 9$ are zero up to the radius of 30 cm and show linear decrease up to the radius of around 75 cm and then exibit quadratic decrease up to the radius of around 84 cm and afterwards they increase. Clearly the magnitudes of f_n for this Orsay field data are almost twice larger than those of the two previous sets of field data and the magnitudes of t_n of this Orsay field data are inbetween those of the two previous sets of data.

Figure 4.14 shows the plots of k_0 and k_n for $n = 3, 6, 9$. The curve of k_0 starts out from zero and increases up to the radius of 84 cm and then decreases sharply. The maximum value is 0.50 which is two times larger than that of the 130 MeV field and three times larger than that of the Harper Cyclotron field. The maximum value of k_3 is 0.20 which is around two times larger than those of the 130 MeV field and the Harper Cyclotron field but what is common is that k_3 decreases for these three sets of field data and the minimum value is -1.0. The maximum value of k_6 is 0.15 which is almost the same as those of the two previous sets of field data and the minimum value is -0.30 which is almost the same as those of the two previous sets of field data.

The maximum value of k_9 is 0.20 which is two times larger than that of the Harper cyclotron field data and almost the same as that of the 130 MeV field data and the minimum value is -0.50 which is almost the same as that of the 130 MeV field data. Refer to the figures of 4.1, 4.2, 4.7, 4.8.

Figure 4.15 shows the plots of $(\Delta E)/E$ and $(-\Delta\tau)/\tau$ both in the units of 10^{-4}. Note that the values of these two quantities are in the units of 10^{-5} for the two previous field data. The reason the value of $(\Delta E)/E$ is very large for small radius is that the energy is almost zero when the radius is small, so the difference is amplified. Both of these show similar patterns of behaviour except that the magnitude of $(\Delta E)/E$ is around twice as large as that of $-(\Delta\tau)/\tau$, which is quite natural (see eq. 4.4). They show the same polarity of fluctuation except for the value of outermost radius where the fractional period difference decreases sharply while the fractional energy difference increases sharply. The absolute differences are 3×10^{-4} for $(\Delta E)/E$ and 1.0×10^{-4} for $-(\Delta\tau)/\tau$ up to the radius of 60 cm and become erratic afterwards. The maximum magnitudes of $(\Delta E)/E$ and $-(\Delta\tau)/\tau$ are almost three to four times larger than those of the two previous sets of data, and this is quite natural because the magnitudes of f_n and k_n of this Orsay field data are about 1.5 to 2 times larger than those of the two previous sets of data (refer to figure 4.1, 4.2, 4.7, 4.8).

Figure 4.16 shows the plots of $\Delta\nu_r$ in the units of 10^{-3} above that of $\Delta(\nu_z^2)$ in the units of 10^{-3}. The reason we have the plot of $\Delta(\nu_z^2)$ instead is that there is a small region of values of radius where the theory shows imaginary values of ν_z , while the E. O. Code shows that, even though being small, the values of ν_z are real. Both of these show rapid change from 70 to 90 cm. Around this range of radius, we observe that the plots of t_3, t_6, and t_9 change more sharply than in the range of radius, $0 \leq r \leq 70$ (cm). As is true for all the field data, the values of $\Delta\nu_r$ and $\Delta\nu_z^2$ are positive, if averaging out the fluctuations. The polarity of the small fluctuations on these curves

is opposite. What is different from the case of the two previous sets of field data is that we can hardly see periodic fluctuations and these two plots of the differences are rather smooth. This is due to the fact that the field data of the Orsay cyclotron were obtained not from the actual measurements of the field but from the numerical calculations. In the case of the two previous sets of data, the plot of $\Delta\nu_r$ is in the units of 10^{-4} and that of $\Delta\nu_z$ is in the units of 10^{-3}. The magnitude of $\Delta\nu_r$ is about five to six times as large as those of the two previous sets of data. This is due to the fact that the magnitudes of f_n and k_n of the Orsay field data are about 1.5 to 2 times larger than those of the two previous sets of data and hence the effect of these terms is squared because the terms in κ_x^2 (refer to eq. 2.15) and $(g_x)_n^2$ (refer to eq. 2.16) are functions of f_n^2 and $f_n k_n$, etc. The magnitude of $\Delta(\nu_z^2)$ is about three to four times larger than those of the two previous sets of data. Because you can't compare $\Delta(\nu_z^2)$ with $\Delta\nu_z$, you should compare $\Delta(\nu_z^2)$ of the Orsay field data with $2\nu_z \times \Delta(\nu_z)$. This is also due to the fact that the magnitudes of f_n and k_n of the Orsay field data are about 1.5 to 2 times larger than those of the two previous sets of data and hence the effect is squared because the terms in κ_z^2 (refer to eq. 2.17) and $(g_z)_n^2$ are functions of f_n^2 and $f_n k_n$. Hence the final effect is the amplification of these differences by a factor of around four.

Figure 4.17 shows the plot of ν_r above that of ν_z. The result obtained from the E. O. Code lies above that from the theory. Note that some of the values obtained from the analytical formulas are negative which, for convenience, indicates that the values are actually imaginary.

Figure 4.18 shows the plot of ν_z obtained from the E. O. Code, that from the theory by M. M. Gordon and that from the theory by Hagedoorn and Verster. As can be seen, the deviation of the values obtained from the theory by Hagedoorn and Verster from those obtained from the E. O. Code is much larger than those obtained from the

theory by M. M. Gordon. The theory by Hagedoorn and Verster predicts imaginary values of ν_z over broad range of the radii where imaginary values are represented by negative values.

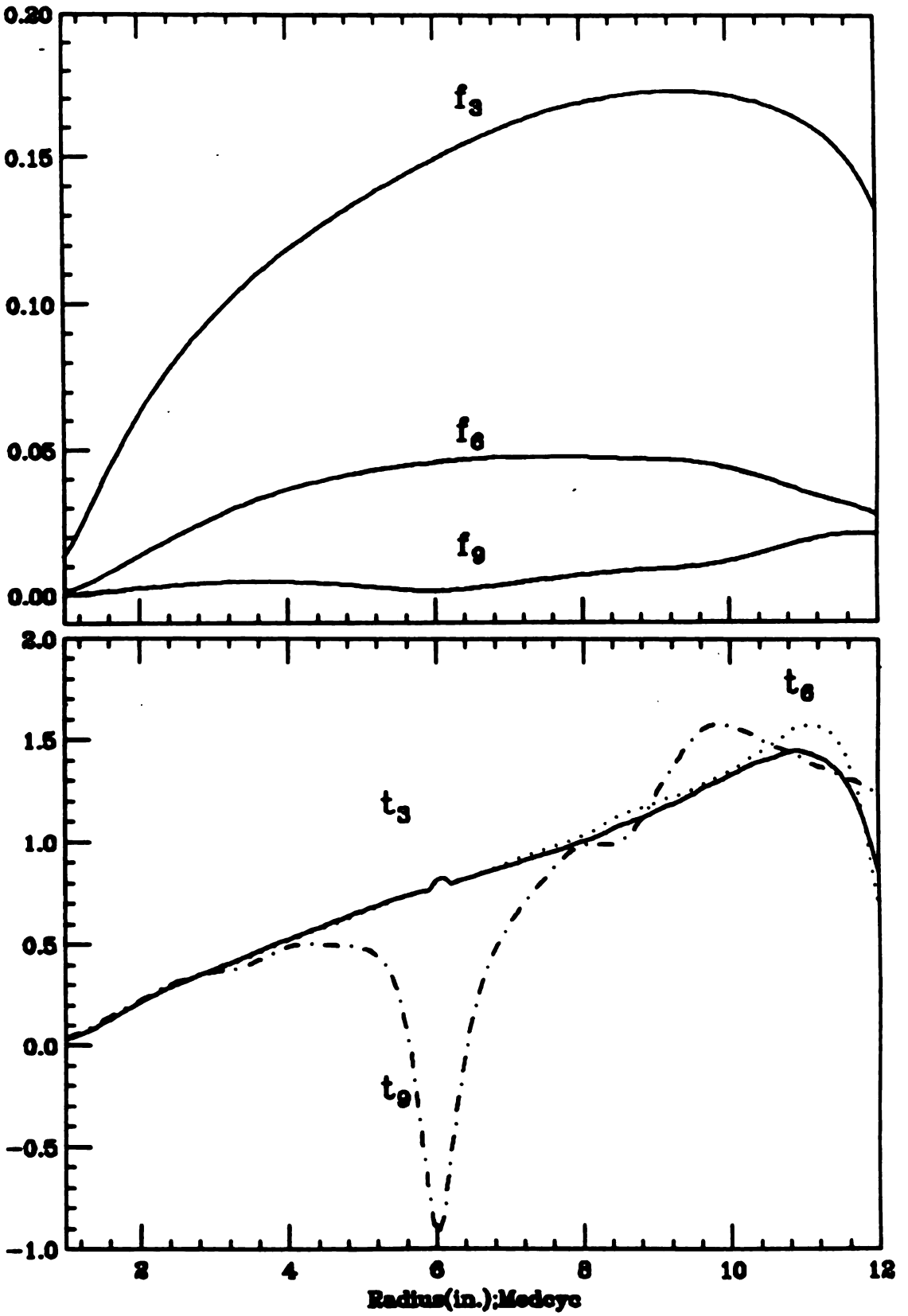

Figure 4.1: Plots of f_n and t_n for $n = 3, 6, 9$ of the Harper cyclotron.
t_3 is depicted with a solid line, t_6 with a dotted line, t_9 with a dotdashed line.

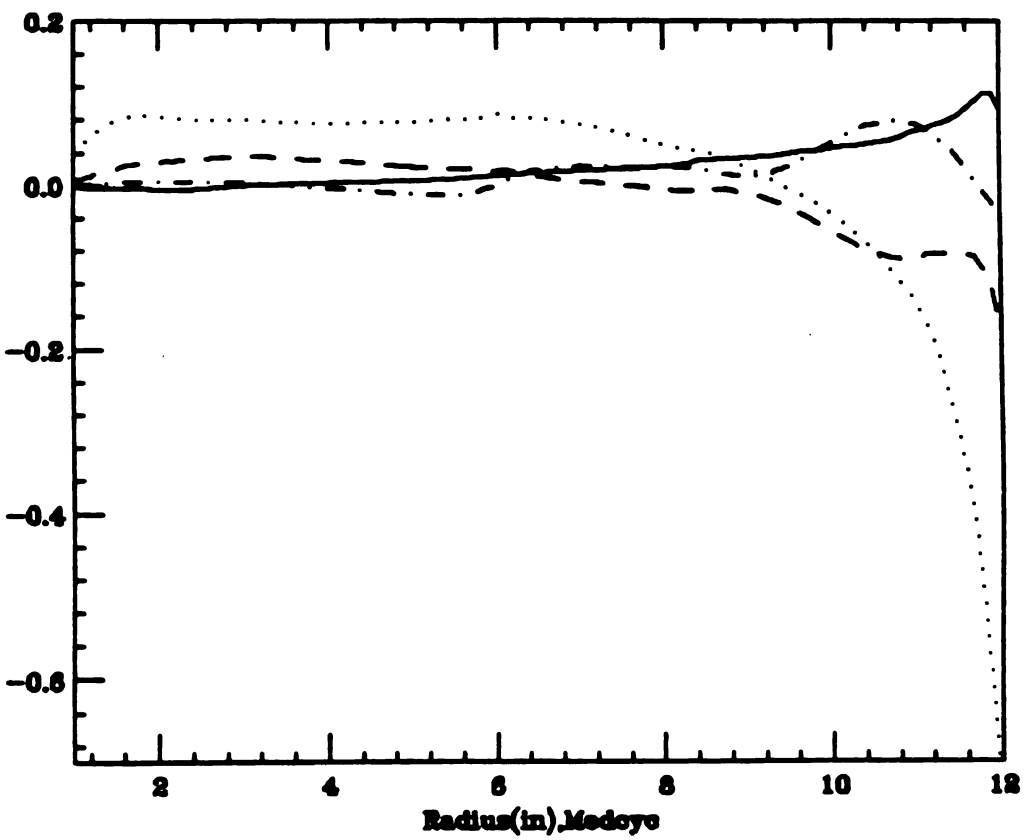

Figure 4.2: Plots of k_n for $n = 0, 3, 6, 9$ of the Harper cyclotron.
k_0 is depicted with a solid line, k_3 with a dotted line, k_6 with a dashed line, k_9 with a dotdashed line.

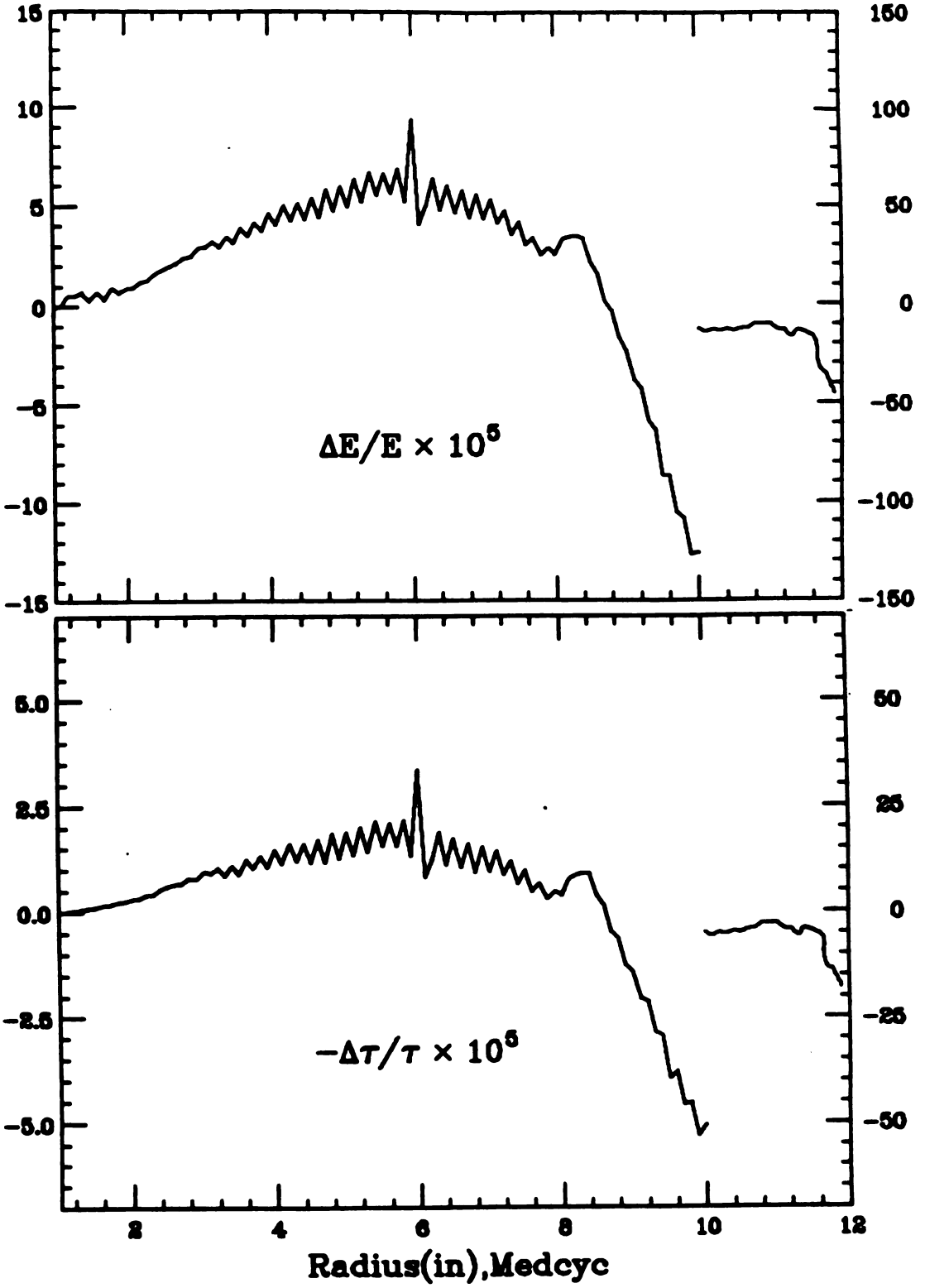

Figure 4.3: Plots of $\Delta E/E$ and $-\Delta\tau/\tau$ of the Harper cyclotron: in units of 10^{-5}. Note there is a change of scale at 10 in. The left scale is valid to the radius of 10 in. and the right scale valid from 10 in. to 12 in.

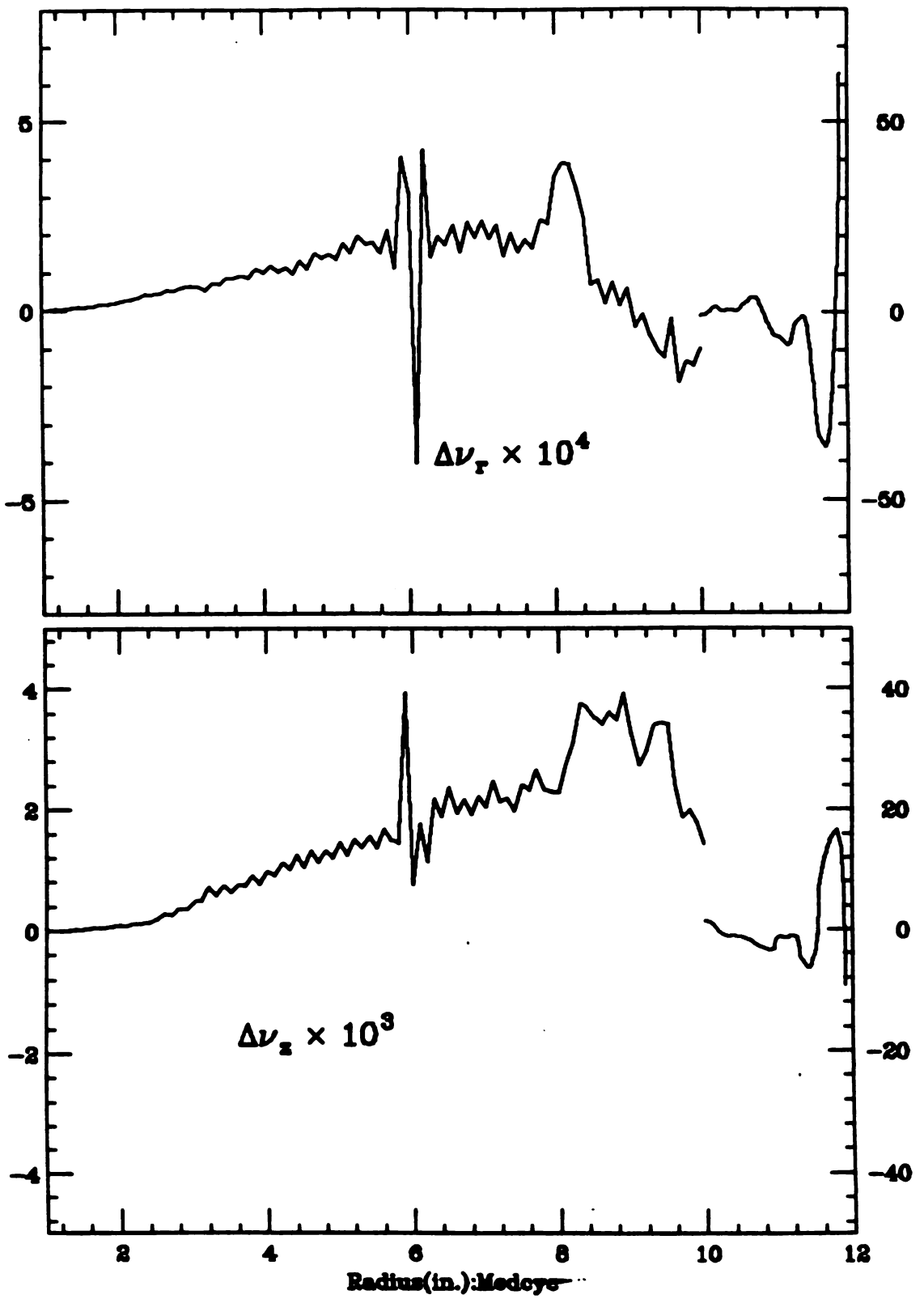

Figure 4.4: Plots of $\Delta\nu_r$ in units of 10^{-4} and $\Delta\nu_z$ in units of 10^{-3} for the Harper cyclotron: Note there is a change of scale at 10 in.

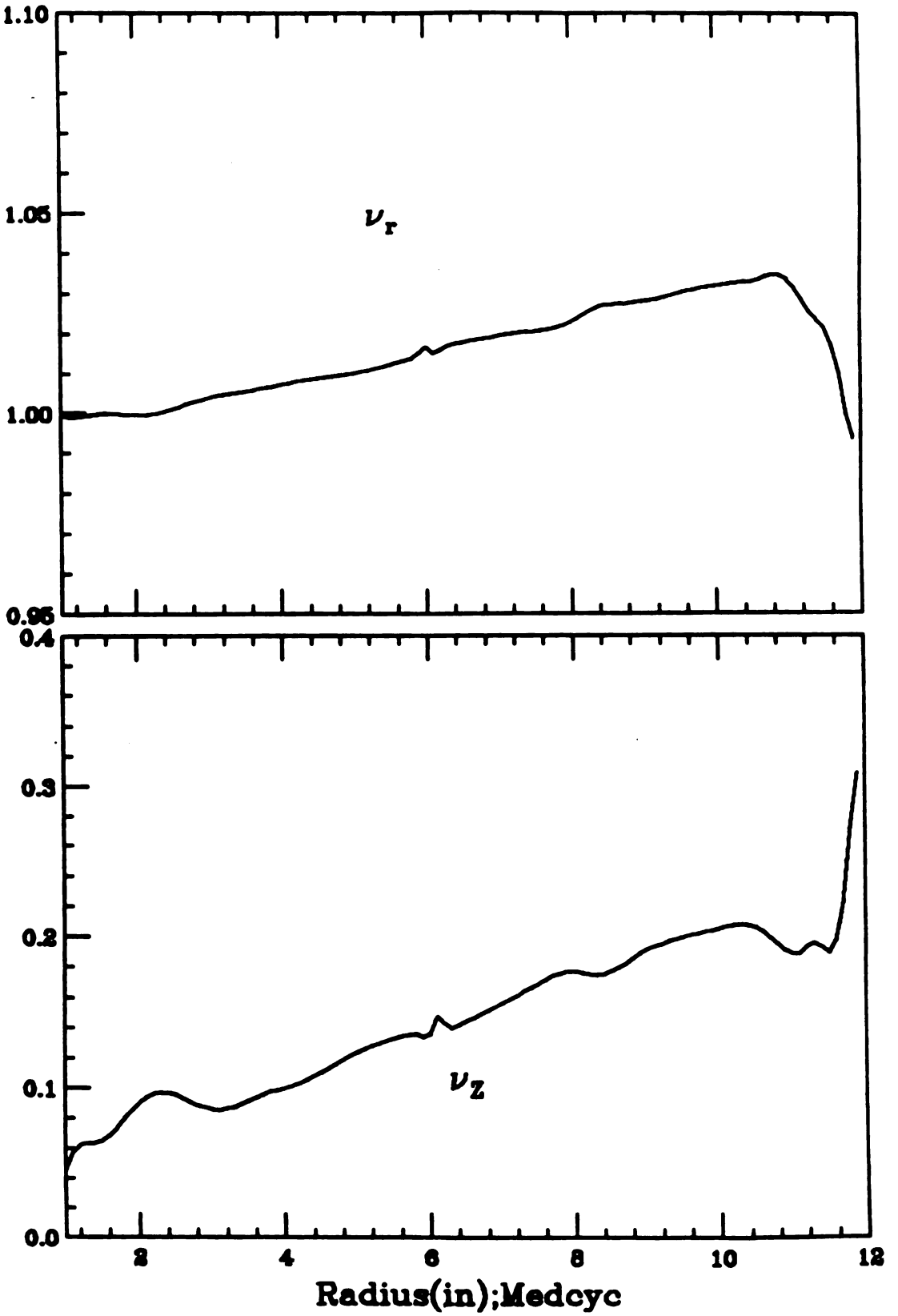

Figure 4.5: Plots of ν_r and ν_z of the Harper cyclotron.
These data are obtained from the E. O. Code.

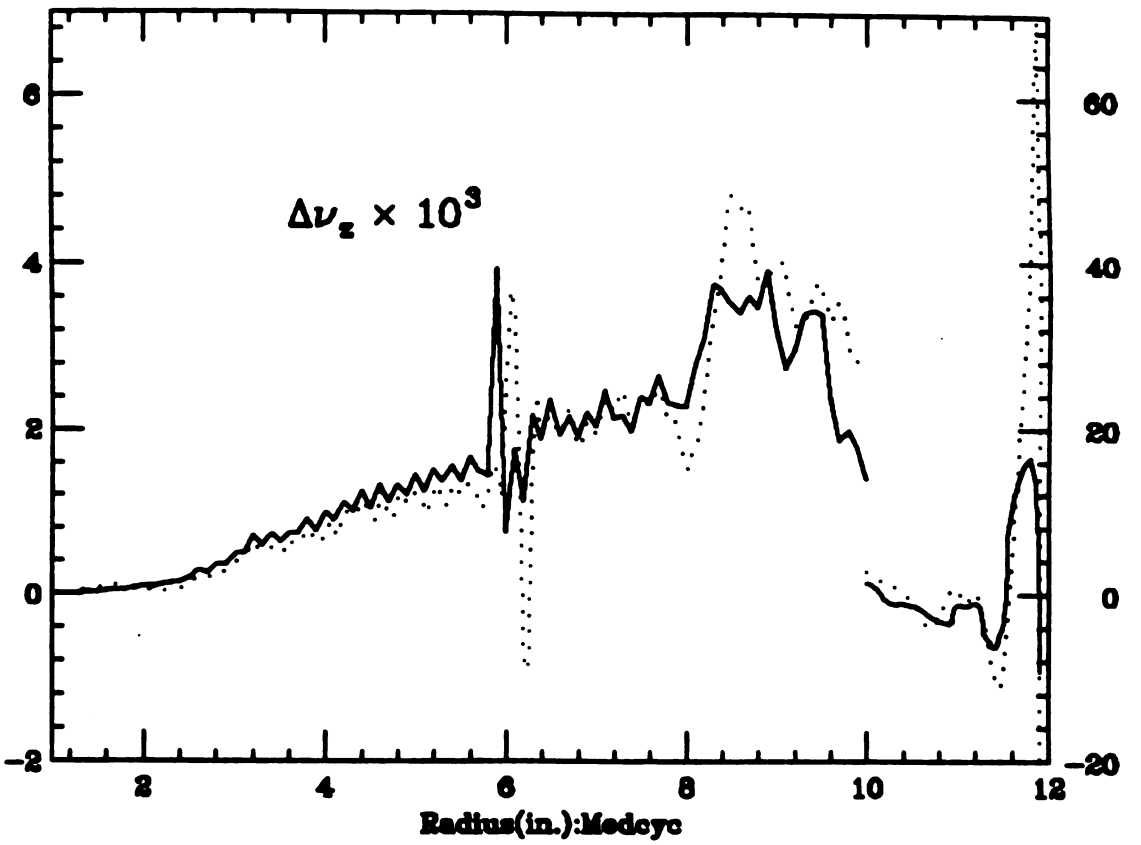

Figure 4.6: Two plots of $\Delta\nu_z$ from two different theories.
The plot of the difference between the ν_z obtained from the E. O. Code and that from the theory by Hagedoorn and Verster is depicted with a dotted line, and that of $\Delta\nu_z$ between the ν_z from the E. O. Code and that from the new theory by M. M. Gordon with a solid line. Note there is a change of scale at 10 in.

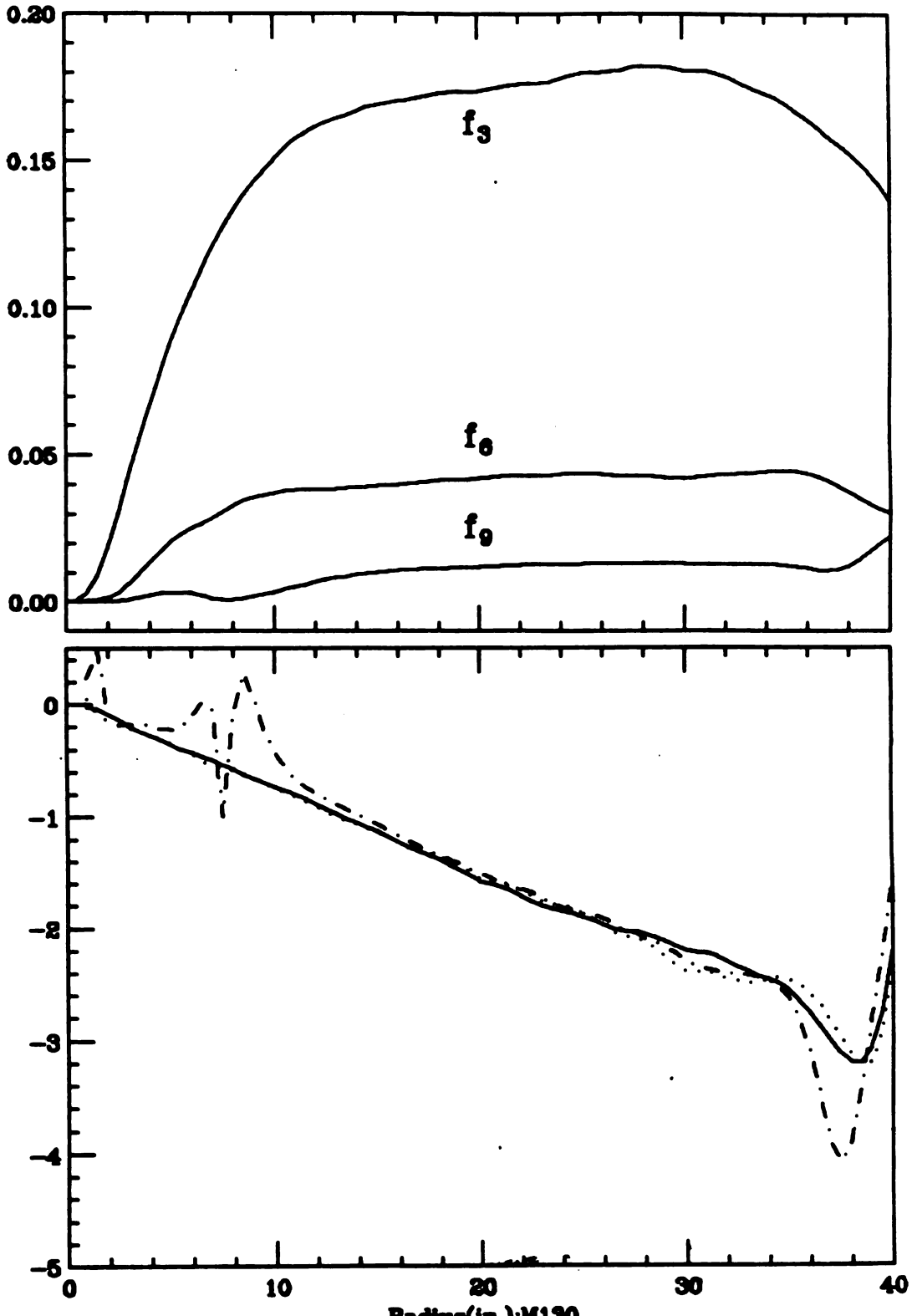

Figure 4.7: Plots of f_n and t_n for $n = 3, 6, 9$ of the 130 MeV/A field data of the MSU K1200 cyclotron: t_3 is depicted with a solid line, t_6 with a dotted line, t_9 with a dotdashed line.

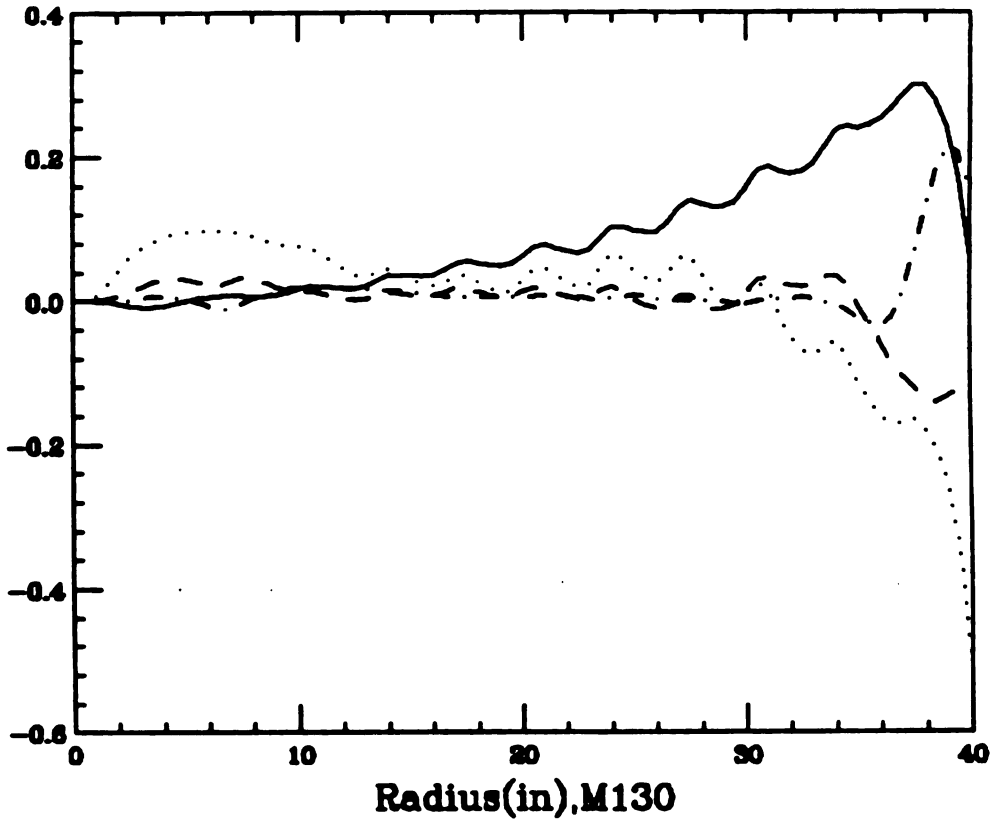

Figure 4.8: Plots of k_n for $n = 0, 3, 6, 9$ of the K1200, 130 MeV/A field.
k_0 is depicted with a solid line, k_3 with a dotted line, k_6 with a dashed line, k_9 with a dotdashed line.

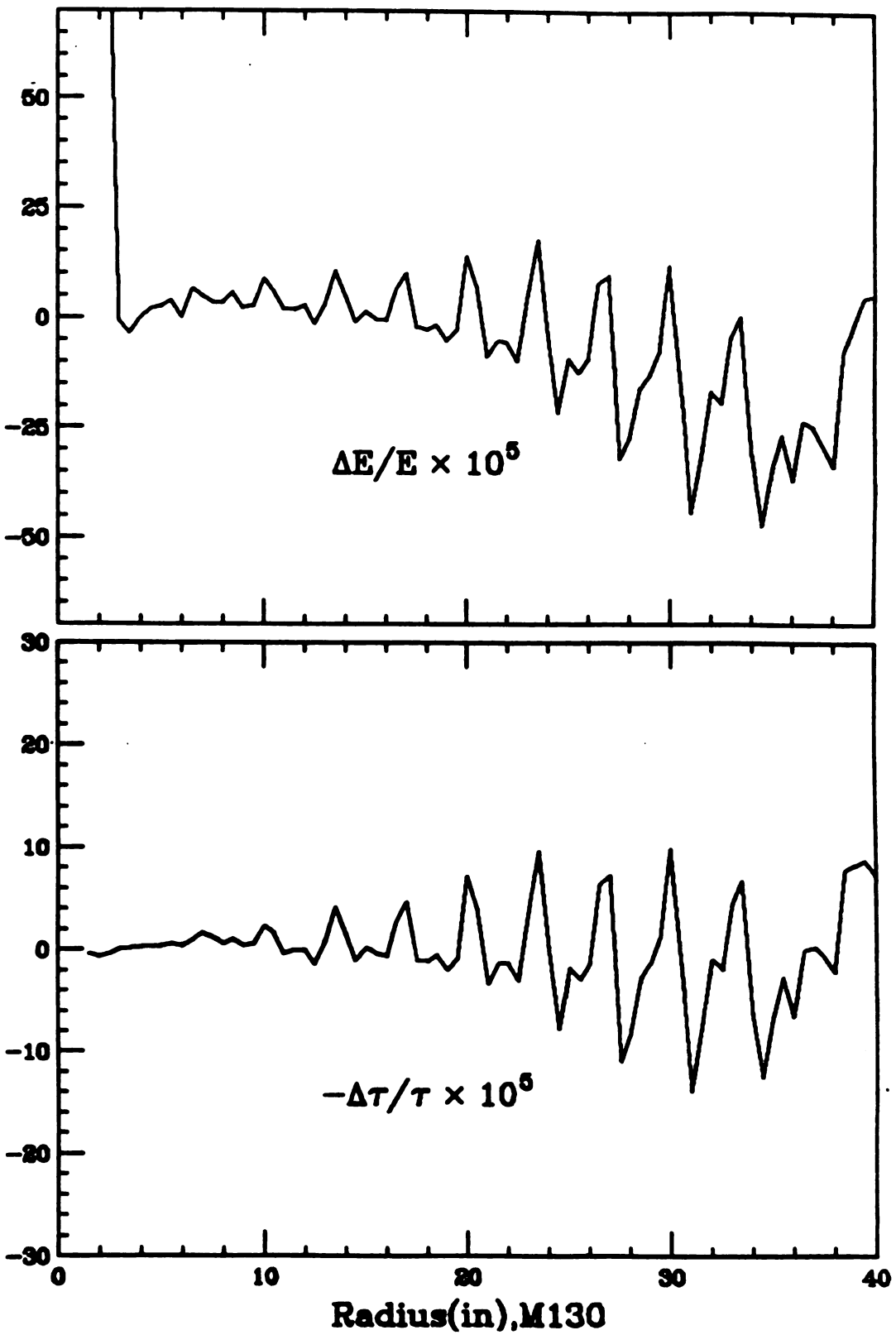

Figure 4.9: Plots of $\Delta E/E$ and $-\Delta\tau/\tau$ of the K1200, 130 MeV/A field: in units of 10^{-5}.

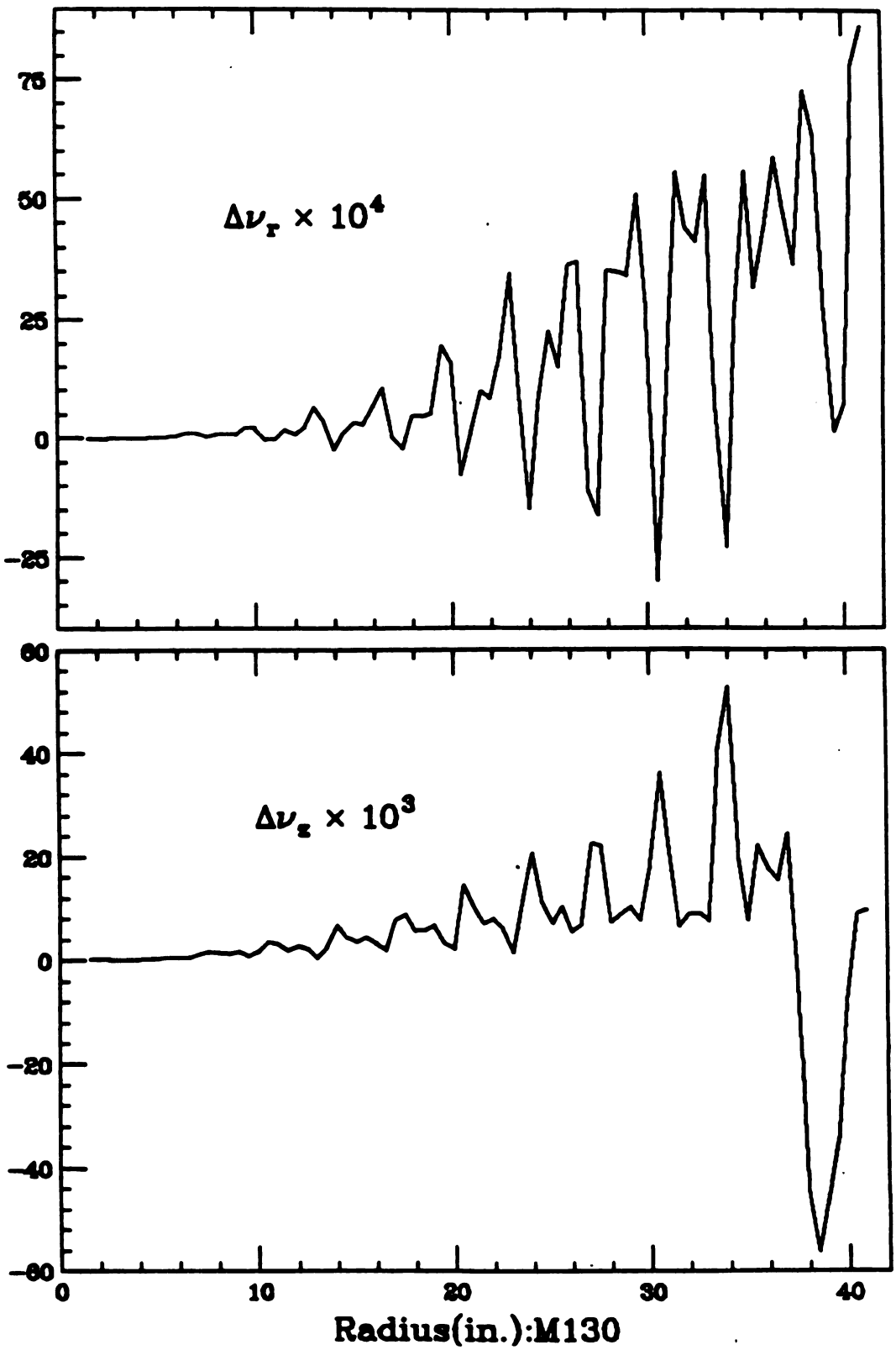

Figure 4.10: Plots of $\Delta\nu_r$ and $\Delta\nu_z$ of the K1200, 130 MeV/A field: $\Delta\nu_r$ is in units of 10^{-4} and $\Delta\nu_z$ in units of 10^{-3}.

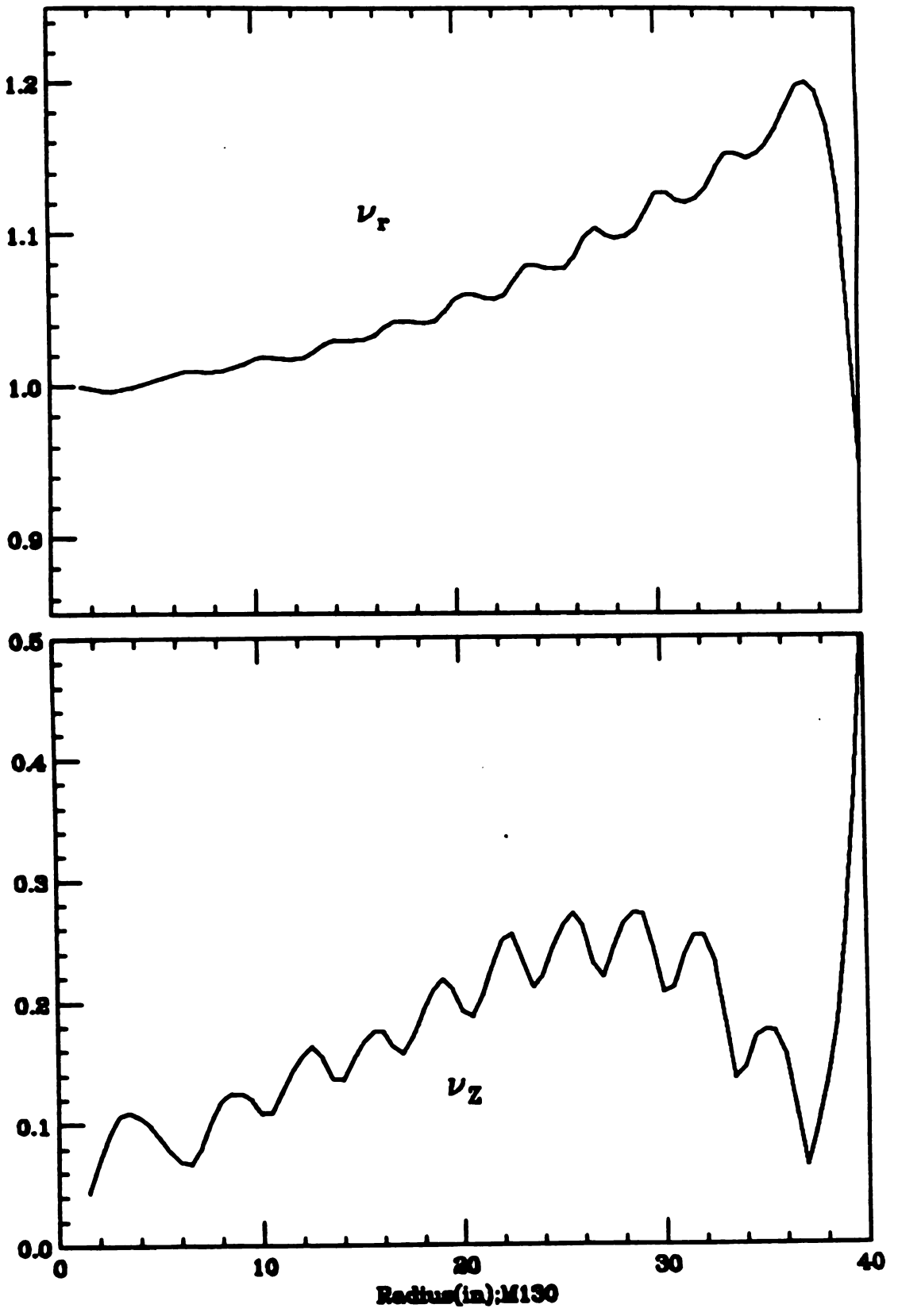

Figure 4.11: Plots of ν_r and ν_z from the E. O. Code for the K1200, 130 MeV/A field.

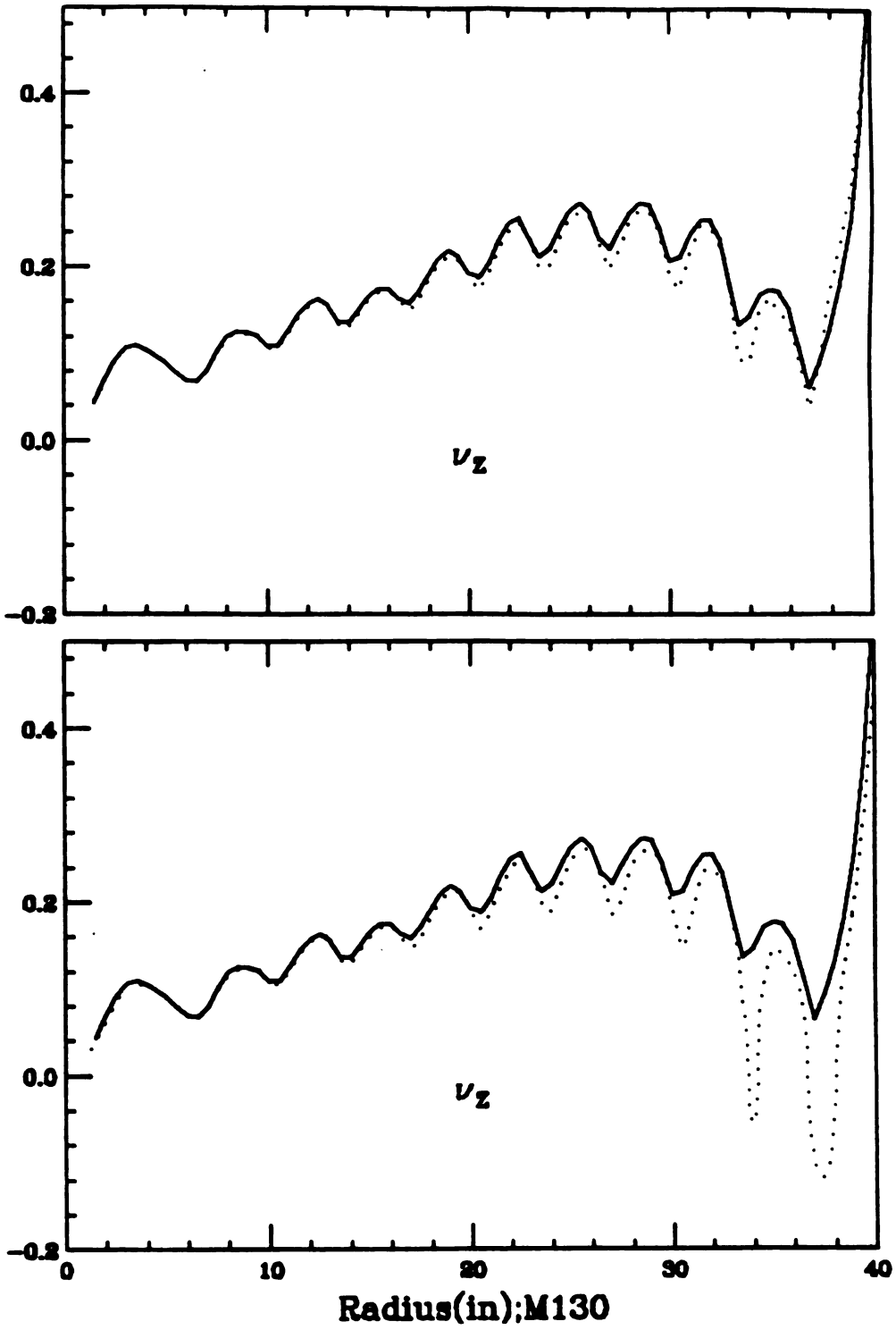

Figure 4.12: Plots of ν_z obtained from the E. O. Code and two different theories for the K1200, 130 MeV/A field data.
Upper scale: The plot of ν_z obtained from the E. O. Code is in a solid line and that from the theory by M. M. Gordon is in a dotted line. Lower scale: The plot of ν_z obtained from the E. O. Code is in a solid line and that from the theory by Hagedoorn and Verster in a dotted line.

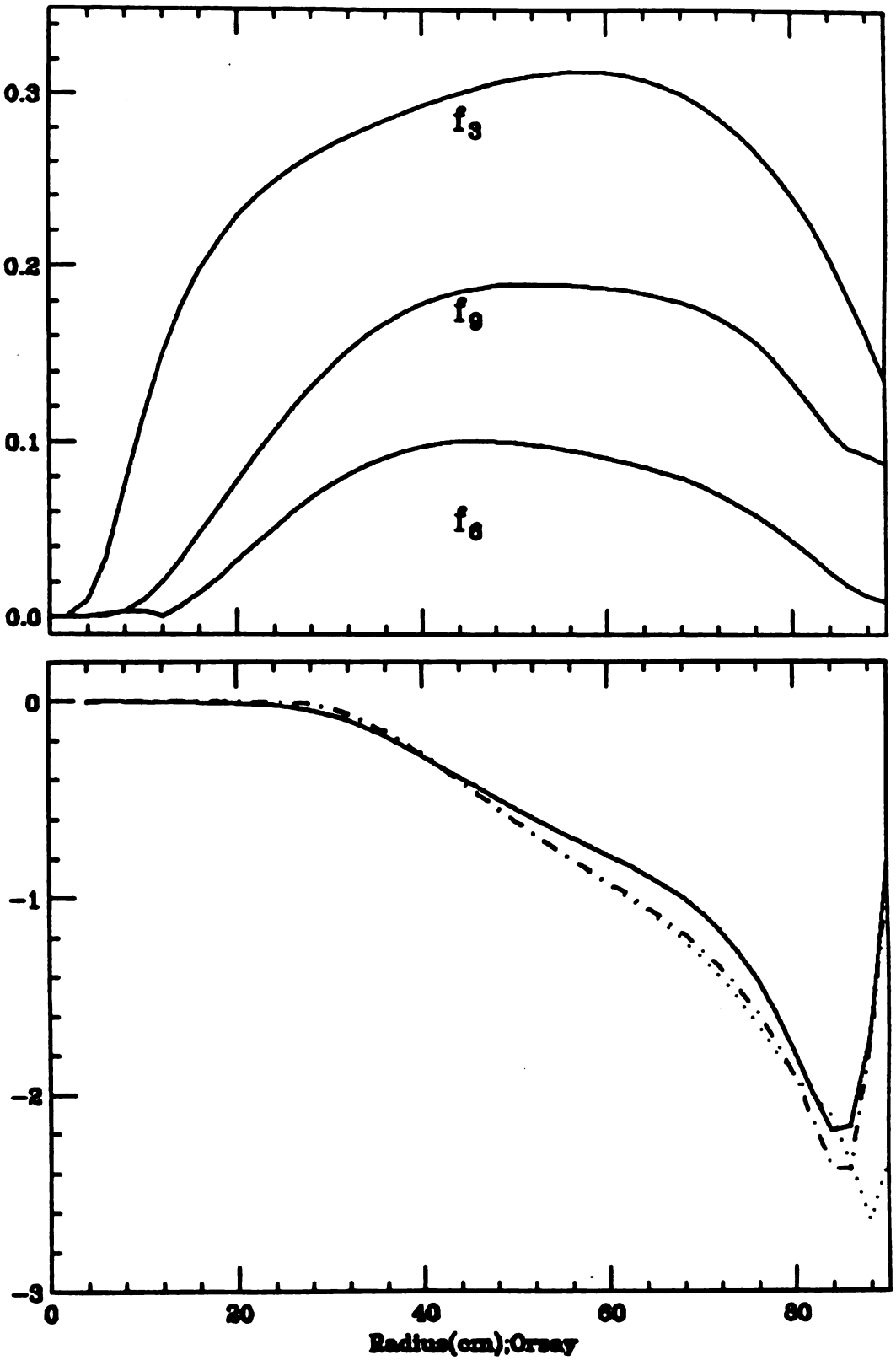

Figure 4.13: Plots of f_n and t_n for $n = 3, 6, 9$ of the Orsay field.
t_3 is depicted with a solid line, t_6 with a dotted line, t_9 with a dotdashed line.

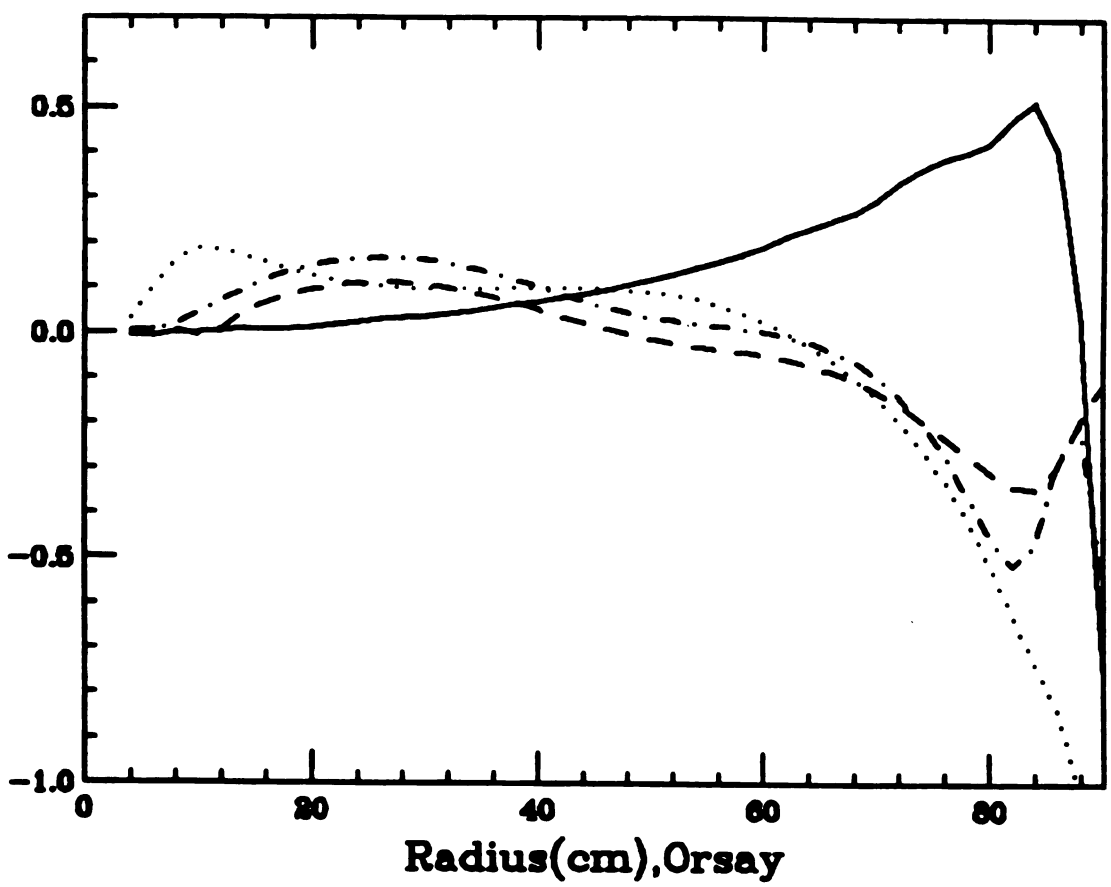

Figure 4.14: Plots of k_n for $n = 0, 3, 6, 9$ of the Orsay field.
k_0 is depicted with a solid line, k_3 with a dotted line, k_6 with a dashed line, k_9 with a dotdashed line.

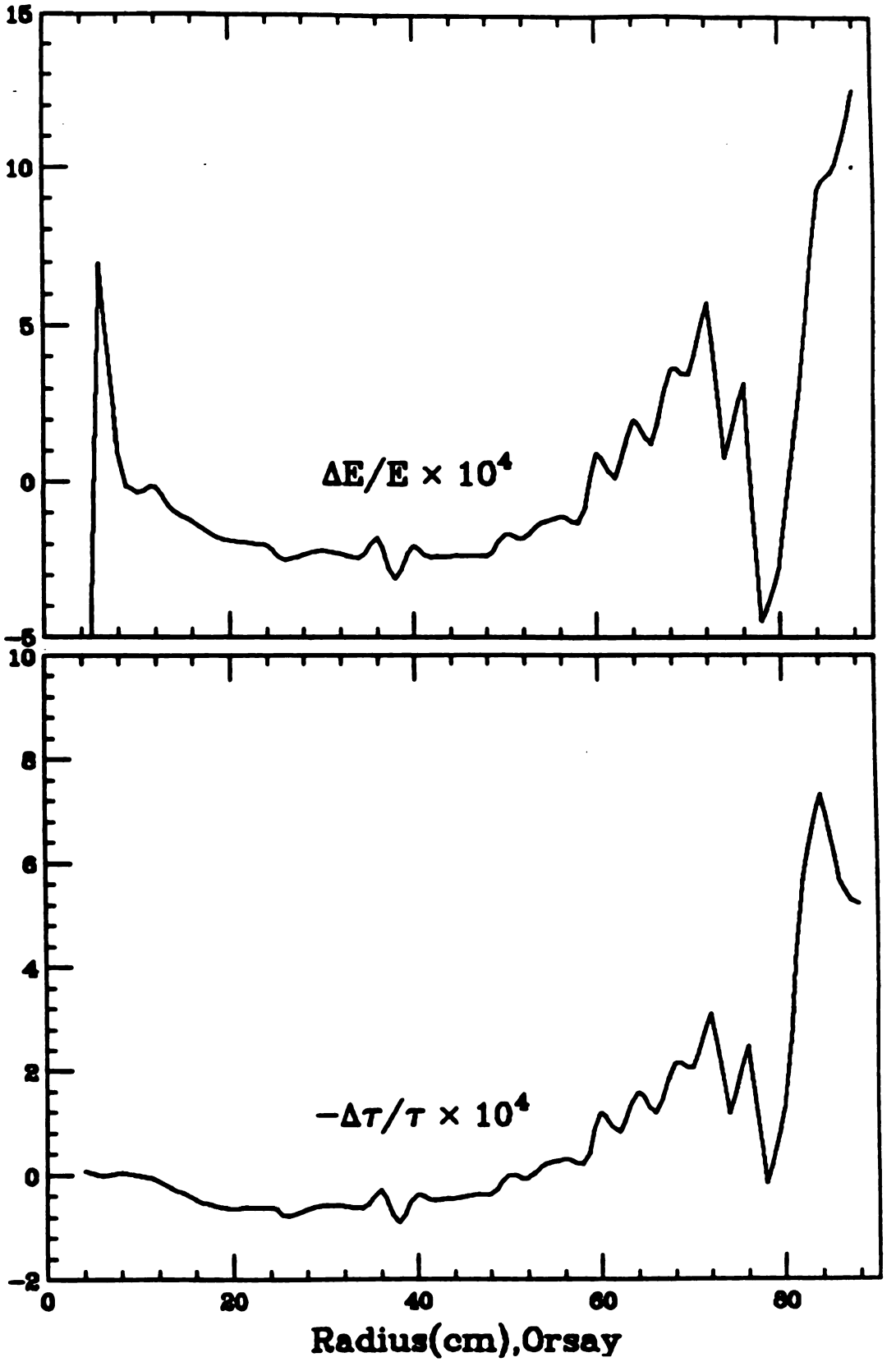

Figure 4.15: Plot of $\Delta E/E$ and $-\Delta\tau/\tau$ of the Orsay field: in units of 10^{-4}.

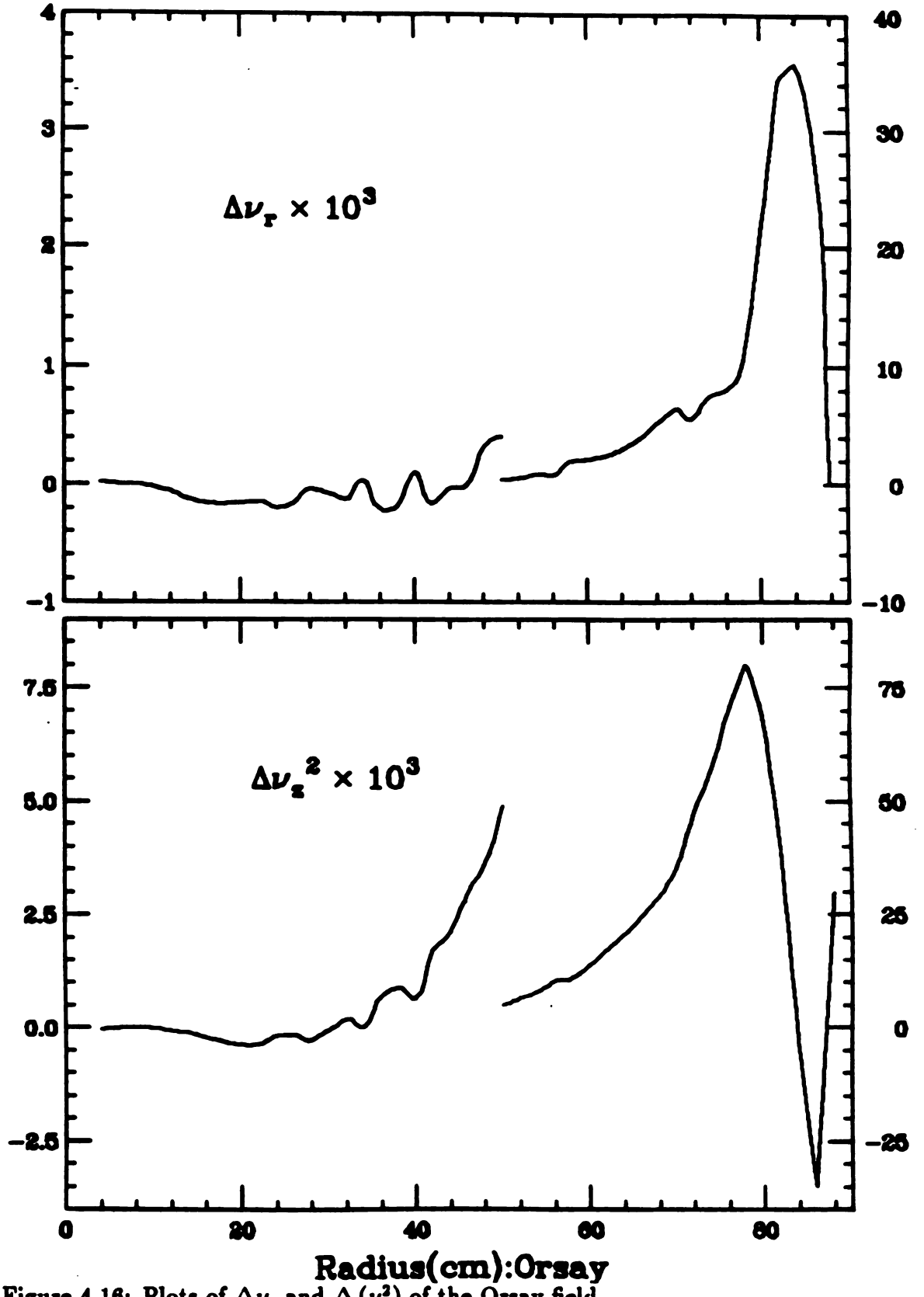

Figure 4.16: Plots of $\Delta\nu_r$ and $\Delta(\nu_z^2)$ of the Orsay field.
Note there is a change of scale at 50 cm.

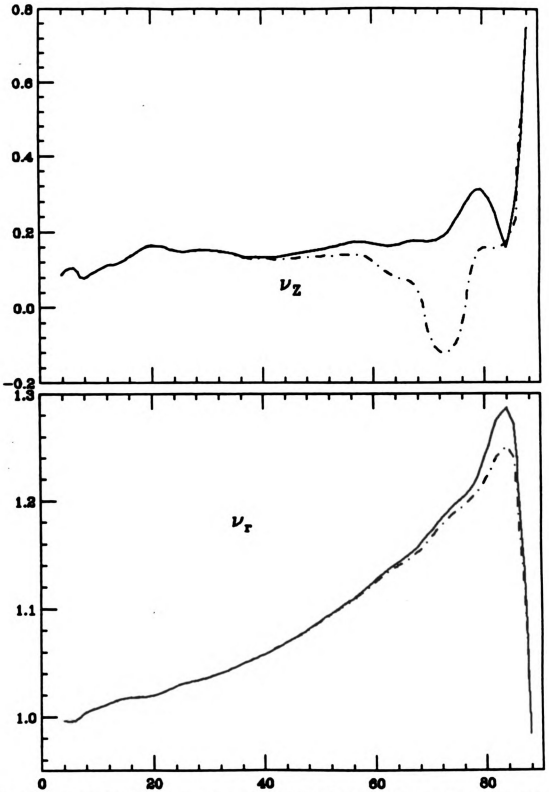

Figure 4.17: Plots of ν_r and ν_z from the E. O. Code and the theory by Gordon for the Orsay field: The tunes obtained from the E. O. Code are depicted with a solid line, and those from the theory by M. M. Gordon depicted with a dotdashed line. The imaginary values of ν_z are represented by negative values.

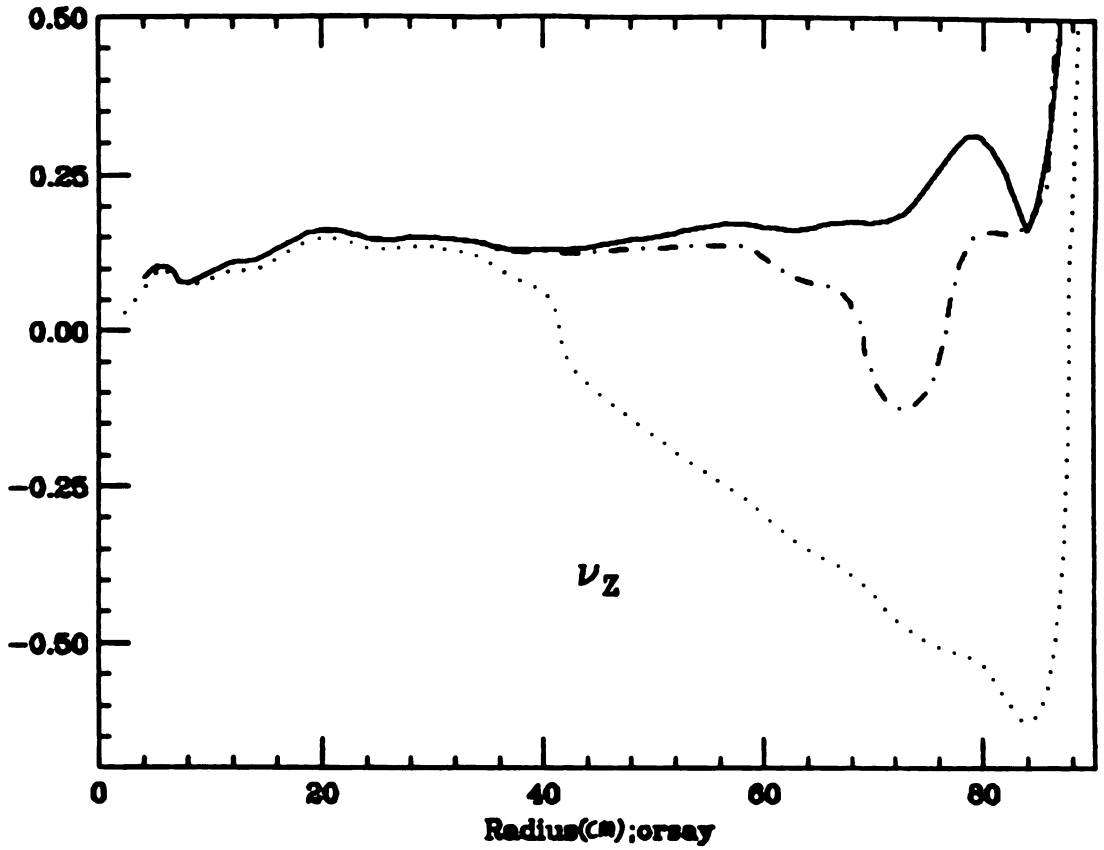

Figure 4.18: Plots of ν_z obtained from the E. O. Code, from the theory by M. M. Gordon and from the theory by Hagedoorn and Verster: The plot of ν_z obtained from the E. O. Code is depicted with a solid line, that from the theory by M. M. Gordon depicted with a dotdashed line and that from the theory by Hagedoorn and Verster depicted with a dotted line.

Chapter 5

Conclusions

For the Harper Cyclotron field, the absolute value of $(\Delta E)/E$ and $(\Delta\tau)/\tau$ are less than 50×10^{-5} and 20×10^{-5} respectively which are fairly small (refer to figure 4.3). The absolute values of $\Delta\nu_r$ and $\Delta\nu_z$ are less than 60×10^{-4} and 20×10^{-3} respectively (refer to figure 4.4). From this, we can say that the matching of the E. O. Code and the theory is very good.

For the 130 MeV field, the absolute value of $(\Delta E)/E$ and $(\Delta\tau)/\tau$ are less than 50×10^{-5} and 25×10^{-5} respectively (refer to figure 4.9), which are quite similar to those above. Also the absolute values of $\Delta\nu_r$ and $\Delta\nu_z$ are less than 80×10^{-4} and 60×10^{-3} respectively (refer to figure 4.10). As can be seen, the absolute values of the differences of the tunes are somewhat larger than those for the Harper Cyclotron field. Neverthcless, the theoretical formulas are still quite good.

In the case of these two sets of field data, the flutter field is relatively small compared with the average field. Hence the assumptions of theory are fairy well satisfied.

For the Orsay field, the absolute values of $(\Delta E)/E$ and $(\Delta\tau)/\tau$ are less than 15×10^{-4} and 8×10^{-4} (refer to figure 4.15), which indicates that the matching of the E. O. Code and the theory is good, but not as good as for the other two cases.

Also the absolute values of $\Delta\nu_r$ and $\Delta(\nu_z^2)$ are less than 40×10^{-3} and 80×10^{-3} (refer to figure 4.16) which are around five times as large as those of the 130 MeV field.

The reason why the results for the Orsay field are worse than those of the Harper Cyclotron field and the 130 MeV field is that the average value of the Orsay field (20 kG) is less than half that of the other two (45 kG). Since the flutter field is about the same for all three, it is relatively more important for the Orsay field so that the assumptions of the theory are less well satisfied.

One result worthy of note is that the theory seems to predict smaller values for both ν_r and ν_z than those obtained form the Equilibrium Orbit Code. This conclusion holds for all three fields investigated here, provided one averages out the fluctuations produced by irregularities in the measured field data.

Appendix A

Appendix by M.M.Gordon

I Field Parameters

We assume that the median plane field $B(r,\theta)$ is given as a function of the polar coordinates r and θ. This function is usually specified in a polar mesh with fixed intervals Δr and $\Delta\theta$. Actually the field is represented by a Fourier series:

$$B(r,\theta) = B_0(r) + \sum_n B_n(r)\cos\left[n(\theta - \beta_n(r))\right] , \tag{A.1}$$

where $B_0(r)$ is the average field, $B_n(r)$ is the amplitude of the n^{th} harmonic, and the function $\theta = \beta_n(r)$ gives the spiral curve for this harmonic. For a cyclotron with N sectors and no imperfections, n takes on the values $n = N, 2N, \ldots$, so that the angular period is $\theta_0 = 2\pi/N$.

Assuming $B_0(r)$, $B_n(r)$, and $\beta_n(r)$ are known, we calculate the following dimensionless parameters:

$$f_n = \frac{B_n}{B_0} , \tag{A.2}$$

$$t_n = r\left(\frac{d\beta_n}{dr}\right) , \tag{A.3}$$

$$k_n = \frac{r}{B_0}\left(\frac{dB_n}{dr}\right) , \tag{A.4}$$

$$k'_n = \frac{r^2}{B_0}\left(\frac{d^2 B_n}{dr^2}\right) , \tag{A.5}$$

where these k_n and k'_n apply for $n = 0$ as well as the other n values. In addition, we need:

$$k''_0 = \frac{r^3}{B_0}\left(\frac{d^3 B_0}{dr^3}\right) . \tag{A.6}$$

All of the above parameters are required at each r value in order to carry out the calculations.

II Equilibrium Orbit Calculation

For a point charge q moving in the median plane with a constant momentum p, the differential equation for the trajectory can be derived from the following Lagrangian:

$$L(r,\dot{r},\theta) = p(\, r^2 + \dot{r}^2\,)^{\frac{1}{2}} - q\int rB(r,\theta)\,dr \tag{A.7}$$

where dots are used to denote θ derivatives so that $\dot{r} = dr/d\theta$, for example.

We assume that the orbit is nearly circular so that $(\dot{r}/r)^2$ is small. Expansion of L then leads to :

$$L(r,\dot{r},\theta) = \frac{1}{2}p\frac{\dot{r}^2}{r} - \int (\, qrB(r,\theta) - p\,)\; dr \tag{A.8}$$

where terms of fourth and higher order terms have been dropped. The resultant differential equation is :

$$\frac{d}{d\theta}\left(\frac{\dot{r}}{r}\right) + \frac{1}{2}\left(\frac{\dot{r}}{r}\right)^2 = 1 - \frac{q}{p}rB(r,\theta) . \tag{A.9}$$

The equation for the equilibrium orbit is written as follows:

$$r_{eo} = r_0\,[\; 1 + y\,(\,\theta\,)\;]^2 \;, \tag{A.10}$$

where $y\,(\,\theta\,)$ has the same periodicity as the field. For simplicity, we take $\langle\; y(\theta)\;\rangle = 0$, and our reference radius r_0 therefore has an unconventional definition:

$$r_0 = \langle\,(\,r_{eo}\,)^{\frac{1}{2}}\;\rangle^2 . \tag{A.11}$$

It is this r_0 which is used as the independent variable in the formulas given below, and it should be clearly understood that for every circle of radius r in the given field, there is an equilibrium orbit having $r = r_0$. The field parameters associated with this value of r_0 then determine the momentum p of the particle and hence the remaining orbit properties.

The differential equation for $y(\theta)$ is then given by:

$$\ddot{y} = \frac{1}{2}(1+y)\left[1 - \frac{q}{p} r B(r,\theta)\right] , \tag{A.12}$$

which is correct at least to second order. Expanding the right side in powers of y, the result is:

$$\ddot{y} = -M - F(\theta) - M'y - F'(\theta)y - \frac{1}{2}M''y^2 - \ldots , \tag{A.13}$$

where we have dropped all terms of third and higher order in the flutter field, that is, the oscillatory part of $B(r,\theta)$. The expansion coefficients are given by:

$$M = \frac{1}{2}(\lambda - 1) , \tag{A.14}$$

$$F(\theta) = \frac{1}{2}\lambda \sum_n f_n \cos(n(\theta - \beta_n)) , \tag{A.15}$$

$$M' = \lambda(1 + k_0) + \frac{1}{2}(\lambda - 1) , \tag{A.16}$$

$$F'(\theta) = \frac{1}{2}\lambda \sum_n [(3f_n + 2k_n)\cos(n(\theta - \beta_n)) + 2n f_n t_n \sin(n(\theta - \beta_n))] , \tag{A.17}$$

$$M'' = \lambda(3 + 7k_0 + 2k_0') \tag{A.18}$$

and where the parameter λ is defined by:

$$\lambda = \frac{q}{p} r_0 B_0(r_0) . \tag{A.19}$$

If the flutter field vanishes so that the field is axially symmetric, then we have only the zero order solution $y^0 = 0$, so that $r_{eo} = r_0$, and $\lambda \equiv 1$, or $p = q r_0 B_0(r_0)$

which is obviously true. The first order value of $y(\theta)$ is obtained by solving:

$$\ddot{y} + M'y = -F(\theta) , \tag{A.20}$$

with the solution given by:

$$y(\theta) = \frac{1}{2}\lambda \sum_n y_n \cos(\, n(\, \theta - \beta_n \,)\,) , \tag{A.21}$$

with $y_n = \frac{f_n}{n^2 - M'}$.

A technique for obtaining an improved solution for $y(\theta)$ will be discussed in a later section. We should note that a more detailed development of the material in this and the following section can be found in a previous paper [8].

III Calculation of p and ω

Since $\langle\ \ddot{y}\ \rangle = 0$, the average value of eq. A.13, above yields:

$$0 = M + \langle\ F'(\theta)y\ \rangle + \frac{1}{2}M''\langle\ y^2\ \rangle . \tag{A.22}$$

Hence we obtain the following formula for λ:

$$1 - \lambda = \frac{1}{4}\lambda^2 \sum_n \left[(\, 3f_n + 2k_n \,)\, y_n + \frac{1}{2}M''y_n^2 \right] . \tag{A.23}$$

Since the right hand side is of second order, an iteration scheme is used to obtain the value of λ and hence p. That is, we start by setting $\lambda = 1$ on the right and use the resultant value of $(\, 1 - \lambda \,)$ for the next approximation and so on. Once λ is found, we obtain the value of p and hence the energy E.

If C is the circumference of the equilibrium orbit, and if τ is the orbit period, then:

$$C = v\tau = 2\pi R . \tag{A.24}$$

Thus we have:

$$R = v/\omega = \langle\, (\, r^2 + \dot{r}^2 \,)^{\frac{1}{2}}\ \rangle , \tag{A.25}$$

where $\omega = 2\pi/\tau$. If ω_0 is a fixed reference frequency, we find:

$$\frac{\omega_0}{\omega} = \frac{r_0\omega_0}{v}\left[\, 1 + \frac{1}{8}\lambda^2 \sum_n (\, 2n^2 + 1\,) y_n^2 \,\right], \tag{A.26}$$

correct to second order. This formula is then used to determine the deviation from the isochronism condition, that is, the condition $\omega = \omega_0$ independent of energy.

In addition to R defined above, it is useful to obtain the average radius given by:

$$\bar{r} = \langle\, r_{eo} \,\rangle = r_0 \left(1 + \frac{1}{8}\lambda^2 \sum_n y_n^2 \right) \tag{A.27}$$

again correct to second order. This $\bar{r}$ is the average radius occurring in the standard output of the equilibrium orbit code.

IV Radial Oscillations

We start from the exact Lagrangian given in eq. A.7 and set:

$$r = r_{eo} + x$$

and

$$\dot{r} = \dot{r}_{eo} + \dot{x} \ .$$

An expansion of the Lagrangian, L, to second order in x and $\dot{x}$ then gives:

$$L = \frac{1}{2}\frac{\dot{x}^2}{a^2} + bx\dot{x} + \frac{1}{2}cx^2 \ , \tag{A.28}$$

where a, b, and c are periodic functions of θ given below. If we now set $x = a\xi$, then L can be transformed into the standard form:

$$L = \frac{1}{2}\dot{\xi}^2 - \frac{1}{2}K(\theta)\xi^2 \tag{A.29}$$

where $K(\theta) = a^2(\, \dot{b} - c\,) - h^2 + \dot{h}$, with $h = \dot{a}/a$

In this case, the equation for the linear oscillations becomes:

$$\ddot{\xi} + K(\theta)\xi = 0 \tag{A.30}$$

and since $K(\theta)$ is periodic, this is a Matthieu - Hill equation.

For the radial oscillations, the parameters a, b, and c are given by:

$$a^2 = (r^2 + \dot{r}^2)^{\frac{3}{2}}/r^2 , \tag{A.31}$$

$$b = -r\dot{r}(r^2 + \dot{r}^2)^{-\frac{3}{2}} , \tag{A.32}$$

$$c = \dot{r}^2(r^2 + \dot{r}^2)^{-\frac{3}{2}} - \frac{q}{p}\left[\frac{\partial}{\partial r}(rB)\right] \tag{A.33}$$

where all quantities are evaluated at $r = r_{eo}(\theta)$ and $\dot{r} = \dot{r}_{eo}(\theta)$. Hence we find:

$$K_x(\theta) = \frac{qr}{p}\left[\frac{\partial}{\partial r}(rB)\right](1 + \frac{\dot{r}^2}{r^2})^{\frac{3}{2}} + \dot{h}_1 - h_1^2 , \tag{A.34}$$

where here, $h_1 = \frac{\dot{a}}{a} - \frac{\dot{r}}{r}$.

This expression for $K_x(\theta)$ is exact, but it must be evaluated along the equilibrium orbit and this can be done only approximately.

We divide $K(\theta)$ into two parts:

$$K(\theta) = \kappa^2 - g(\theta) \tag{A.35}$$

where $\langle K(\theta) \rangle = \kappa^2$ so that $\langle g(\theta) \rangle = 0$. Thus $g(\theta)$ is the oscillatory part and contains the alternating gradient focusing. If κ^2 is calculated to second order, then $g(\theta)$ should be obtained only to first order since its contribution to the focusing is then of second order.

For the radial motion specifically, a detailed calculation gives the following values:

$$g_x(\theta) = -\lambda\sum_n (nf_nt_n)\sin(n(\theta - \beta_n)) -$$

$$\lambda\sum_n \left[f_n + k_n + \lambda y_n(1 + 3k_0 + k_0') + \frac{1}{2}n^2y_n \right]\cos(n(\theta - \beta_n)) \tag{A.36}$$

and

$$\kappa_x^2 = \lambda(1+k_0) + \frac{1}{2}\lambda^2 \sum_n y_n \left(f_n + 3k_n + k_n' - n^2 f_n t_n^2 \right) +$$

$$\frac{1}{8}\lambda^2 (6\lambda(1+k_0) - 1) \sum_n n^2 y_n^2 +$$

$$\frac{1}{8}\lambda^3 (1 + 11k_0 + 11k_0' + 2k_0'') \sum_n y_n^2 \, . \qquad \text{(A.37)}$$

It is these quantities that are used to calculate ν_r, the radial tune.

In the limit of large N values, we obtain the simple smooth (or high frequency) approximation value:

$$g_x(\theta) \longrightarrow -\sum_n (n f_n t_n) \sin(n(\theta - \beta_n)) \, , \qquad \text{(A.38)}$$

$$\kappa_x^2 \longrightarrow 1 + k_0 - \frac{1}{2}\sum_n f_n^2 t_n^2 \, . \qquad \text{(A.39)}$$

Thus g_x reduces to the alternating gradient focusing produced by the spiral , while κ_x^2 reduces to the constant gradient focusing term and a negative term corresponding to Laslett focusing (or defocusing here).

V Vertical Oscillations

Considering only the linear oscillations, the equation of motion for z is:

$$\frac{d}{d\theta}\left(\frac{p\dot{z}}{\sqrt{r^2 + \dot{r}^2}} \right) = q \left[r\frac{\partial B}{\partial r} - \frac{\dot{r}}{r}\frac{\partial B}{\partial \theta} \right] z \, , \qquad \text{(A.40)}$$

which corresponds to the following Lagrangian:

$$L = \frac{1}{2}\frac{\dot{z}^2}{a^2} + \frac{1}{2}cz^2 \, , \qquad \text{(A.41)}$$

where $a^2 = (r^2 + \dot{r}^2)^{\frac{1}{2}}$ and $c = \frac{q}{p}\left[r\frac{\partial B}{\partial r} - \frac{\dot{r}}{r}\frac{\partial B}{\partial \theta} \right]$. The motion here is directly analogous to that of the previous section.

Changing variables from z to ζ such that $z = a\zeta$, the Lagrangian can then be tranformed into standard form:

$$L = \frac{1}{2}\dot{\zeta}^2 - \frac{1}{2}K_z(\theta)\zeta^2 \ , \tag{A.42}$$

where $K_z(\theta) = -a^2c + \dot{h} - h^2$, where $h = \dot{a}/a$. Using the above values for a and c, we then find the following exact form of $K_z(\theta)$:

$$K_z(\theta) = \frac{q}{p}\left[\dot{r}\frac{\partial B}{\partial \theta} - r^2\frac{\partial B}{\partial r} \right]\left(1 + \frac{\dot{r}^2}{r^2} \right)^{\frac{1}{2}} + \dot{h} - h^2 \ . \tag{A.43}$$

Here again all quantities must be evaluated along the equilibrium orbit which can only be done approximately.

The Matthieu - Hill equation for ζ then becomes

$$\ddot{\zeta} + K_z(\theta)\zeta = 0 \ . \tag{A.44}$$

We again separate K_z into two terms:

$$K_z(\theta) = \kappa_z^2 - g_z(\theta) \ , \tag{A.45}$$

where $\langle\ K_z(\theta)\ \rangle = \kappa_z^2$. If we then evaluate $g_z(\theta)$ to first order and κ_z^2 to second order, the following values are obtained:

$$\begin{aligned} g_z(\theta) \ &= \ \lambda\sum_n n f_n t_n \sin\left(n\left(\theta - \beta_n \right) \right) + \\ &\qquad \lambda\sum_n \left(k_n + \lambda y_n\left(2k_0 + k_0' \right) + \frac{1}{2}n^2 y_n \right)\cos\left(n\left(\theta - \beta_n \right) \right) \ , \end{aligned} \tag{A.46}$$

and

$$\begin{aligned} \kappa_z^2 \ &= \ -\lambda k_0 + \frac{1}{2}\lambda^2\sum_n y_n\left(n^2 f_n + n^2 f_n t_n^2 - 2k_n - k_n' \right) - \\ &\qquad \frac{1}{8}\lambda^2\left(1 + 2\lambda k_0 \right)\sum_n n^2 y_n^2 - \frac{1}{8}\lambda^3\left(6k_0 + 9k_0' + 2k_0'' \right)\sum_n y_n^2 \ . \end{aligned} \tag{A.47}$$

If we again consider the limit of large N values, these become

$$g_z(\theta) \longrightarrow \sum_n n f_n t_n \sin\left(n\left(\theta - \beta_n\right)\right) , \tag{A.48}$$

$$\kappa_z^2 \longrightarrow -k_0 + \frac{1}{2}\sum_n f_n^2 + \frac{1}{2}\sum_n f_n^2 t_n^2 . \tag{A.49}$$

We again have the alternating gradient term in $g_z(\theta)$ and the combined effects of constant gradient, Thomas, and Laslett focusing in κ_z^2. The more complete formulas above (and in the sec. IV) show additional focusing effects of gradients in both the flutter field and the average field that become important in the edge region of the magnet.

VI Born Approximation

The Matthieu - Hill equation encountered in the preceding two sections can be written:

$$\ddot{x} + \kappa^2 x = g(\theta)x , \tag{A.50}$$

where $g(\theta)$ is periodic so that $g(\theta + \theta_0) = g(\theta)$, where $\theta_0 = 2\pi/N$. We choose a Green's function $G(\theta, \theta')$ which is a solution when the right side is replaced by a delta function $\delta(\theta - \theta')$ so that:

$$\begin{aligned} G(\theta,\theta') &= 0 \quad , if \theta < \theta' \\ G(\theta,\theta') &= \frac{1}{\kappa}\sin\kappa(\theta - \theta') \quad , if \theta > \theta' . \end{aligned} \tag{A.51}$$

In this case, the general solution becomes:

$$x(\theta) = x^0(\theta) + \frac{1}{\kappa}\int_0^\theta \sin\left(\kappa\left(\theta - \theta'\right)\right) g(\theta') x(\theta')\, d\theta' , \tag{A.52}$$

and

$$\dot{x} = \dot{x}^0(\theta) + \int_0^\theta \cos\left(\kappa\left(\theta - \theta'\right)\right) g\left(\theta'\right) x\left(\theta'\right)\, d\theta' , \tag{A.53}$$

where $x^0(\theta)$ and its derivative $\dot{x}^0(\theta')$ are the zero order values.

We use two independent solutions $x_1(\theta)$ and $x_2(\theta)$ to construct the transfer matrix:

$$M(\theta) = \begin{pmatrix} x_1(\theta) & x_2(\theta) \\ \dot{x}_1(\theta) & \dot{x}_2(\theta) \end{pmatrix} , \tag{A.54}$$

with initial conditions chosen so that $M(\theta = 0) = I$, the unit matrix. Thus we take:

$$x_1^0(\theta) = \cos\kappa\theta , \tag{A.55}$$

$$x_2^0(\theta) = \frac{1}{\kappa}\sin\kappa\theta . \tag{A.56}$$

When these values are inserted into eq. A.54 above, we then obtain x_1 and x_2 at all θ values.

The tune, ν, is obtained from the trace of M at $\theta = \theta_0$:

$$\begin{aligned} 2\cos(\nu\theta_0) &= Tr[\,M(\theta_0)\,] \\ &= x_1(\theta_0) + \dot{x}_2(\theta_0) . \end{aligned} \tag{A.57}$$

Using the solutions given above, we then find:

$$\begin{aligned} 2\cos(\nu\theta_0) = 2\cos\kappa\theta_0 + \frac{1}{\kappa}\int_0^{\theta_0} & g(\theta')\sin(\kappa(\theta_0-\theta'))\,x_1(\theta') + \\ & \cos(\kappa(\theta_0-\theta'))\,x_2(\theta')\;d\theta' . \end{aligned} \tag{A.58}$$

Thus, if $g(\theta) = 0$, we find $\nu = \kappa$, as expected.

If x_1 and x_2 are calculated to first order in $g(\theta)$ using the eq. A.58 above, we obtain $\cos(\nu\theta_0)$ correct to second order:

$$\begin{aligned} 2\cos(\nu\theta_0) = 2\cos(\kappa\theta_0) + \frac{\sin\kappa\theta_0}{\kappa}\int_0^{\theta_0} & g(\theta')\,d\theta' + \\ \frac{1}{\kappa^2}\int_0^{\theta_0} & g(\theta')\int_0^{\theta'} g(\theta'')\sin(\kappa(\theta'-\theta'')) \\ & \times\sin(\kappa(\theta_0-\theta'+\theta''))\,d\theta' d\theta'' . \end{aligned} \tag{A.59}$$

We should note that this expression gives the exact result when $g(\theta)$ corresponds to the focusing produced by two thin lenses located within the sector.

For the case of interest here, we can write:

$$g(\theta) = \sum_n g_n \cos\left(n\theta + \gamma_n \right) \tag{A.60}$$

with $g_0 = \langle\, g(\theta) \,\rangle = 0$ so that the first order term in $\cos\left(\nu\theta_0 \right)$ vanishes. A straightforward but tedious calculation of the integrals yields for this case:

$$\cos\left(\nu\theta_0 \right) = \cos\left(\kappa\theta_0 \right) - \frac{1}{4}\theta_0 \left(\frac{\sin\kappa\theta_0}{\kappa} \right) \sum_n \frac{g_n^2}{n^2 - 4\kappa^2} \,. \tag{A.61}$$

Using the half-angle formula, the alternative form is obtained:

$$\sin^2\left(\nu\theta_0/2 \right) = \sin^2\left(\kappa\theta_0/2 \right) + \frac{1}{8}\theta_0^2 \frac{\sin\kappa\theta_0}{\kappa\theta_0} \sum_n \frac{g_n^2}{n^2 - 4\kappa^2} \,. \tag{A.62}$$

We should note that the above formula can be used not only below the stop-band ($\nu < N/2$), but also within the stop-band where $|\cos\nu\theta_0| > 1$. Also the singularity in the term with $n = N$ where $\kappa = N/2$ is cancelled by the factor $\sin\kappa\theta_0$ in front. That is, in the limit $\kappa \longrightarrow N/2$ and $\kappa\theta_0 \longrightarrow \pi$, we have:

$$\frac{\sin\kappa\theta_0}{N^2 - 4\kappa^2} \longrightarrow \frac{\pi}{2N^2} \tag{A.63}$$

which is finite.

The above formula can also be used when $\kappa^2 < 0$ simply by setting $\kappa = i\,|\kappa|$. That is, by making the following changes:

$$\cos\kappa\theta_0 \longrightarrow \cosh\,|\kappa|\,\theta_0 \,, \tag{A.64}$$

$$sin^2\left(\kappa\theta_0/2 \right) \longrightarrow -sinh^2\left(|\kappa|\,\theta_0/2 \right) \,, \tag{A.65}$$

$$\frac{\sin\kappa\theta_0}{\kappa\theta_0} \longrightarrow \frac{\sinh\,|\kappa|\,\theta_0}{|\kappa|\,\theta_0} \,. \tag{A.66}$$

It often happnes that the vertical oscillations are characterized by quite small values of κ_z^2 as well as ν_z^2. In such cases, the above formulas simplify to:

$$\nu_z^2 \approx \kappa_z^2 + \frac{1}{2}\sum_n \frac{g_n^2}{n^2} \ . \tag{A.67}$$

This formula shows why the most important terms in g_n^2 are those proportional to n^2. Also, this formula leads directly to the smooth approximation result when use is made of the values given in eq. A.67, namely,

$$\nu_z^2 = -k_0 + \frac{1}{2}\sum_n f_n^2 \left(1 + 2t_n^2\right) \ . \tag{A.68}$$

Of course, this result could be improved by using the more complete formulas for κ_z^2 and $g_z(\theta)$ given in eq. A.62.

VII Equilibrium Orbit Improvement

To improve the value of $y(\theta)$ given in eq. A.13, we consider the linear terms:

$$\ddot{y} + [\ M' + F'(\theta)\ ]\, y = \ - F(\theta) \ . \tag{A.69}$$

The homogeneous part of this equation has a particular (Floquet) solution given by:

$$y_f = w(\theta) \exp\left(\, i\mu\phi(\theta)\,\right) \tag{A.70}$$

where $w(\theta)$ and $[\ \phi(\theta) - \theta\ ]$ are real and periodic with the same periodicity as the field. The "tune" here is μ which can be calculated using the formulas in the preceding section by setting $\kappa^2 = M'$ and $g(\theta) = -F'(\theta)$, where M' and $F'(\theta)$ are given in eq. A.16 and eq. A.17.

The function w and ϕ can be obtained from :

$$w^2\dot{\phi} \ = \ 1 \tag{A.71}$$

$$\ddot{w} + [\ M' + F'(\theta)\ ]\, w \ = \ \mu^2/w^3 \ . \tag{A.72}$$

Note that if $F'(\theta) = 0$, then $w = 1$, $\phi = \theta$, and $\mu^2 = M'$. These then are the zero-order values.

To obtain the required solution of the inhomogeneous equation above, we change variables from $y(\theta)$ to $\eta(\phi)$ using a Floquet transformation:

$$y(\theta) = w(\theta)\eta(\phi) \tag{A.73}$$

where η is the solution of:

$$\frac{d^2\eta}{d\phi^2} + \mu^2\eta = -w^3(\theta)F(\theta) \; . \tag{A.74}$$

These equations could, in principle, be used to determine the equilibrium orbit at least to second order.

For simplicity, we treat here only the first order solution. That is, we set $w = 1$, $\phi = \theta$, and obtain as a result the exact same $y(\theta)$ as given in eq. A.21, but with y_n now given by:

$$y_n = \frac{f_n}{n^2 - \mu^2} \; . \tag{A.75}$$

That is, M' is now replaced by μ^2 which can be calculated as described above. Since μ^2 differs from M' by the inclusion of second order terms, it should improve the results. We should also note that all the formulas given in the preceding sections are in terms of y_n rather than its explicit form so that either expression can be used.

References

[1] M.M. Gordon, Particle Accelerators **16** (1984) 39.

[2] L. Smith and A.A. Garren, Lawrence Berkeley Lab.,UCRL Report #8598, January, 1959.

[3] G. Parzen, Ann. of Phys. **15** (1961) 22.

[4] H.L. Hagedoorn and N.F. Verster, Nucl. Instrum. Methods **18,19** (1962) 201.

[5] Samuel D. Conte and Carl de Boor, *Elementary Numerical Analys - an algorithmic approach*, McGraw-Hill,New York, 1980.

[6] H.Blosser et.al.,*Advances in Superconducting Cyclotrons at MSU*, 11th int. Conf. on Cyclotrons and their applications (1986) 157.

[7] S.Galès for Agor project group, *Agor A Superconducting Cyclotron For Light And Heavy Ions*, 11th int. Conf. on Cyclotrons and their Applications (1986) 184.

[8] M.M. Gordon, *Calculation of Isochronous Fields for Sector-focused Cyclotrons*, Particle Accelerators **13** (1983) 67.